PROCEEDINGS OF SCIENCE

TASI 2022 Lectures on Flavor Physics

Wolfgang Altmannshofer[a]

[a] *Department of Physics and Santa Cruz Institute for Particle Physics, University of California, Santa Cruz, CA 95064, USA*

E-mail: waltmann@ucsc.edu

These notes correspond to the lectures on flavor physics given at TASI 2022. After a basic introduction to the concept of flavor in the Standard Model and beyond, we discuss the determination of the flavor parameters in the Standard Model, i.e. the quark and lepton masses as well as the CKM matrix elements. The Standard Model flavor puzzle and possible ways to address it are briefly mentioned as well. Finally, we discuss in more detail a particular class of flavor-changing processes that have played a prominent role in flavor physics in the past several years: B meson decays. We cover both charged current tree-level decays, which are typically used for the determination of CKM matrix elements, as well as neutral current loop-level decays, which are sensitive probes of new physics.

Theoretical Advanced Study Institute (TASI 2022)
6 June - 1 July, 2022
University of Colorado, Boulder

PoS(TASI2022)001

Contents

1. Introduction

The Standard Model matter content consists of three generations of up-type quarks (u, c, t), three generations of down-type quarks (d, s, b), three generations of charged leptons (e, μ, τ), and three generations of neutrinos (ν_1, ν_2, ν_3). Flavor physics is a branch of particle physics that aims at understanding the characteristic properties of the different generations of quarks and leptons and the transitions among them.

Historically, flavor physics had a very significant impact on the development of the Standard Model. A few examples include

- The observed rate of the rare kaon decay $K_L \to \mu^+\mu^-$ was far below the theoretical expectation at the time and led to the prediction of the charm quark [1, 2].

- The discovery of CP violation in the kaon sector led to the prediction of the third generation of quarks [3].
- The measurement of the $B^0 - \bar{B}^0$ oscillation frequency was used to predict the top quark mass (see e.g. [4–8] and many others).

In the current era, flavor physics plays an important role in the search for new physics. Many flavor transitions can be predicted with high accuracy in the Standard Model. Comparing the predictions with experimental results can give indirect insight into physics beyond the Standard Model.

On the one hand, if experiments and the Standard Model agree, constraints on new physics models can be derived. In particular, the size of new sources of flavor violation can be bounded, which has potentially important implications for new physics model building. Constraints from flavor observables and from direct searches at colliders are complementary. Flavor probes are only effective if the new physics has flavor-changing couplings, but their reach to high masses is not limited by the center of mass energy of colliders.

On the other hand, discrepancies between the experimental data and Standard Model predictions can be interpreted as indirect signs of new physics. Establishing a new physics origin of potential discrepancies could have a transformative impact on the field. It would lead to a new mass scale in particle physics which may provide a new target for future direct searches at colliders.

On the experimental side, the most important players in flavor physics at the moment are the LHCb experiment at the LHC [9, 10] and the Belle II experiment at KEK [11]. LHCb is a dedicated b physics experiment with a broad program covering many important flavor processes, including, among many others, rare decays of B mesons, CP violation in B_s mixing, CP violation in the charm sector, and the determination of the CKM angle γ. Also the general-purpose detectors at the LHC, ATLAS and CMS, are making important contributions with regards to b physics, for example, in the search for prominent rare decays like $B_s \to \mu^+\mu^-$ [12, 13].

Belle II is the successor of the Belle experiment, one of two B factories, the other being BaBar. The B factories BaBar and Belle confirmed the Standard Model CKM picture of flavor and CP violation. Many of their accomplishments are summarized in [14]. As BaBar and Belle, the Belle II experiment is a detector at an asymmetric electron-positron collider with a center-of-mass energy at the $\Upsilon(4S)$ resonance that primarily decays into a pair of B mesons. Belle II aims to accumulate nearly 2 orders of magnitude more data than Belle. Its main physics goal is the search for new physics in flavor transitions of B mesons (as well as other mesons and tau leptons) and the precise measurement of CKM parameters.

In addition, there are many smaller experiments that focus on specific flavor-changing processes. Examples include the NA62 experiment at CERN [15, 16] that aims at the observation and precision measurement of the rare kaon decay $K^+ \to \pi^+\nu\bar{\nu}$, the K0TO experiment at JPark [17, 18] that is searching for the corresponding neutral version $K_L \to \pi^0\nu\bar{\nu}$, the MEG II experiment at PSI [19] that is searching for the lepton flavor violating decay $\mu \to e\gamma$, or the mu2e experiment at Fermilab [20] which can improve the sensitivity to μ to e conversion in nuclei by several orders of magnitude.

Looking further into the future, one can expect impactful flavor programs at future particle colliders. Of particular interest are circular electron-positron colliders running on the Z pole, as the proposed FCC-ee [21, 22] and CEPC [23, 24]. The Z pole runs of FCC-ee and CEPC would result in

an unprecedented data sample of more than 10^{12} Z bosons decaying to all types of bottom-flavored and charm-flavored hadrons and tau leptons, enabling a rich flavor physics program and giving access to flavor changing processes that cannot be studied either at LHCb or Belle II.

Flavor physics will remain an important field of research for the foreseeable future. In the absence of direct discoveries of new particles at the LHC, the indirect search for new physics using flavor transitions will arguably become even more important in the coming years. Flavor physics might give the first hints for physics beyond the Standard Model and thus guide future developments in particle physics.

These notes are structured in the following way: Section 2 gives a basic introduction to the concept of flavor in the Standard Model and beyond. We discuss the sources of flavor violation in the Standard Model and their properties, as well as the strong constraints on new physics that can be derived from measurements of flavor transitions. Section 3 focuses on the determination of the flavor parameters in the Standard Model, i.e. the quark and lepton masses as well as the CKM matrix elements. In section 4, the Standard Model flavor puzzle and possible ways to address it are discussed briefly. Finally, in section 5, we discuss in more detail a particular class of flavor-changing processes that have played a prominent role in flavor physics in the past several years: B meson decays. We cover both charged current tree-level decays, which are typically used for the determination of CKM matrix elements, as well as neutral current loop-level decays, which are sensitive probes of new physics.

Overall, these notes follow very closely the lectures given at TASI in June 2022. The section 5.5 on the rare B decay anomalies has been updated to reflect the recent experimental results on the lepton flavor universality ratios R_K and R_{K^*} by LHCb. Other excellent TASI lectures on flavor physics and lectures from other summer schools include [25–32]. Additional useful resources for flavor physics are the Heavy Flavor Averaging Group (HFLAV) [33], which provides regular updates to the world averages of heavy flavor quantities, and the Flavour Lattice Averaging Group (FLAG) [34], which reviews lattice results relevant for flavor physics.

These notes do not cover the physics of neutrinos. Recent lecture notes on neutrino physics can, for example, be found in [35, 36].

2. Flavor in the Standard Model and Beyond

2.1 Flavor Breaking in the Standard Model and the CKM Matrix

We start with a reminder of the Standard Model matter content. The Standard Model quarks and leptons are organized in five different representations of the gauge group $SU(3)_c \times SU(2)_L \times U(1)_Y$

$$Q_j = (3, 2, \frac{1}{6}), \quad U_j = (3, 1, \frac{2}{3}), \quad D_j = (3, 1, -\frac{1}{3}), \quad L_j = (1, 2, -\frac{1}{2}), \quad E_j = (1, 1, -1). \tag{1}$$

Each of these representations comes in three generations or flavors, i.e. the generation/flavor index runs over $j = 1, 2, 3$.

The kinetic terms of the fermions in the Standard Model Lagrangian are flavor universal

$$\mathcal{L}_{\text{SM}} \supset \sum_{\Psi} \sum_{j} \bar{\Psi}_j i \not{D} \Psi_j \,. \tag{2}$$

Here, the sum over $\Psi = Q, U, D, L, E$ corresponds to the sum over the fermion "types" and $j = 1, 2, 3$ sums over the flavors. The kinetic terms are invariant under a large global flavor symmetry

$$G_{\text{flavor}} = U(3)^5 = U(3)_Q \times U(3)_U \times U(3)_D \times U(3)_L \times U(3)_E \,, \tag{3}$$

corresponding to individual $U(3)$ flavor rotations for each of the fermion types. It is convenient to split each $U(3)$ symmetry into a $SU(3)$ symmetry that contains the non-trivial flavor mixing and a $U(1)$ factor. One can write

$$G_{\text{flavor}} = SU(3)_Q \times SU(3)_U \times SU(3)_D \times SU(3)_L \times SU(3)_E \times U(1)^5 \,. \tag{4}$$

The $U(1)^5$ factor contains, for example, baryon number and lepton number.

The flavor symmetry is explicitly broken by the Standard Model Yukawa couplings

$$\mathcal{L}_{\text{SM}} \supset -\sum_{j,k} \left[(Y_u)_{jk} \bar{Q}_j U_k \tilde{H} + (Y_d)_{jk} \bar{Q}_j D_k H + (Y_e)_{jk} \bar{L}_j E_k H \right] \; + \; \text{h.c.} \,. \tag{5}$$

The Yukawa couplings $(Y_u)_{jk}, (Y_d)_{jk}, (Y_e)_{jk}$ are, in principle, generic 3×3 matrices in flavor space. In the above expression, H is the Higgs doublet. After electroweak symmetry breaking, we expand the Higgs around its vacuum expectation value (vev) $\langle H \rangle = \frac{1}{\sqrt{2}} \begin{pmatrix} 0 \\ v \end{pmatrix}$. This gives rise to quark and lepton mass terms

$$(\hat{m}_u)_{jk} = \frac{v}{\sqrt{2}} (Y_u)_{jk} \,, \quad (\hat{m}_d)_{jk} = \frac{v}{\sqrt{2}} (Y_d)_{jk} \,, \quad (\hat{m}_e)_{jk} = \frac{v}{\sqrt{2}} (Y_e)_{jk} \,. \tag{6}$$

The standard approach is to switch to a flavor basis in which the mass terms are real and diagonal, the mass eigenstate basis. This is accomplished by a well-known procedure in which the Yukawa couplings / mass terms are diagonalized using bi-unitary transformations. The quark and lepton masses are then given by the eigenvalues of the Yukawa matrices $(Y_u)_{jk}, (Y_d)_{jk}, (Y_e)_{jk}$. The remnant of the bi-unitary transformations is the Cabibbo-Kobayashi-Maskawa (CKM) quark mixing matrix V [3, 37], which appears in the charged current interactions of the quarks

$$\mathcal{L}_{\text{SM}} \supset \frac{g}{\sqrt{2}} V_{jk} \bar{u}_j \gamma^\mu P_L d_k W^+_\mu \; + \; \text{h.c.} \,. \tag{7}$$

In this expression, g is the $SU(2)_L$ gauge coupling, u_j and d_k are up and down quark mass eigenstates of flavor j and k, and V_{jk} are the CKM matrix elements. As is well known, the CKM matrix is a unitary 3×3 matrix which is fixed by 4 free parameters (more in section 3.2).

2.2 Flavor-Changing Neutral Currents

In contrast to the charged current interactions involving the W boson shown above in equation (7), all neutral current interactions in the Standard Model remain flavor diagonal at the tree level. This is the case both for the gauge interactions of the gluons, photon, and Z boson, and the interactions of the Higgs boson. One says there are no flavor-changing neutral currents (FCNCs) in the Standard Model at the tree level.

In the case of the gauge bosons, this is a consequence of the flavor universality of the gauge interactions and the unitarity of the quark mixing. The fact that the Higgs couplings in the Standard

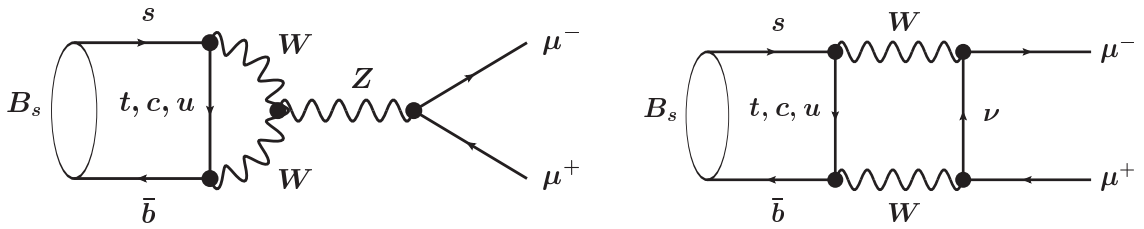

Figure 1: Example 1-loop diagrams that contribute to the decay $B_s \to \mu^+\mu^-$ in the Standard Model.

Model are flavor-conserving is a consequence of the minimal electroweak symmetry-breaking sector that contains only a single Higgs doublet.

Historically, the absence of FCNCs at the tree level was explained by the Glashow, Iliopoulos, Maiani (GIM) mechanism [1], which introduced the charm quark and thus enabled a unitary mixing among the quarks.

Flavor-changing neutral currents do arise at the loop level. One distinguishes between $\Delta F = 1$ processes, where flavor quantum numbers change by one unit, and $\Delta F = 2$ processes, where flavor quantum numbers change by two units.

An example of a $\Delta F = 1$ process is the leptonic decay of the B_s meson, $B_s \to \mu^+\mu^-$. The B_s is a bound state of a strange quark and an anti-bottom quark, and thus "bottom number" and "strange number" change by one unit: $|\Delta B| = |\Delta S| = 1$. Example 1-loop diagrams are shown in figure 1. The diagram on the left is known as a "penguin diagram", and the one on the right is a "box diagram". Penguin diagrams refer to diagrams with flavor-changing vertex corrections[1].

Without performing the actual 1-loop calculation, we can understand the generic structure of the corresponding decay amplitude. We have

$$A(B_s \to \mu^+\mu^-) \propto G_F \frac{g^2}{16\pi^2} \sum_{i=u,c,t} V_{is}^* V_{ib} f(x_i)\,, \quad \text{with } x_i = \frac{m_i^2}{m_W^2}\,. \tag{8}$$

The expression for the amplitude contains the Fermi constant G_F because the decay is mediated by the weak interactions, a loop factor $g^2/16\pi^2$, a loop function f that depends on the mass of the quark in the loop, and the CKM factors $V_{is}^* V_{ib}$ corresponding to the quarks involved. The sum is over all the up-quark flavors that can run in the loop.

Writing out the sum explicitly, we have in the example at hand, but generically also for any $b \to s$ transition,

$$\begin{aligned} A(b \to s) &\propto V_{us}^* V_{ub} f(x_u) + V_{cs}^* V_{cb} f(x_c) + V_{ts}^* V_{tb} f(x_t) \\ &= V_{ts}^* V_{tb}\big(f(x_t) - f(x_c)\big) + V_{us}^* V_{ub}\big(f(x_u) - f(x_c)\big) \\ &\simeq V_{ts}^* V_{tb}\big(f(x_t) - f(0)\big) = V_{ts}^* V_{tb} \tilde{f}(x_t)\,, \end{aligned} \tag{9}$$

with $\tilde{f}(0) = 0$. In the second line, we used the CKM unitarity $V_{us}^* V_{ub} + V_{cs}^* V_{cb} + V_{ts}^* V_{tb} = 0$, and in the third line, we used the smallness of the charm and up quarks $x_u, x_c \ll 1$.

[1] If you wonder where the name penguin diagram comes from, the story is beautifully told in a symmetry magazine article [38].

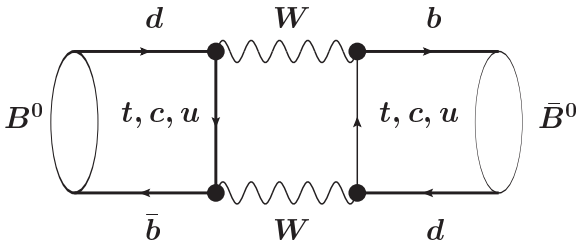

Figure 2: Example 1-loop diagram that contributes to $B^0 - \bar{B}^0$ oscillations in the Standard Model.

Equation (9) illustrates another aspect of the GIM mechanism [1]: If all up-quark masses were equal, $x_t = x_c = x_u$, flavor changing neutral currents would be absent also beyond tree level. The large mass of the top quark results in a large amount of "GIM breaking" and relatively sizable 1-loop contributions to $b \to s$ decays and analogously also to $b \to d$ decays.

For $s \to d$ transtions, for example $K_L \to \mu^+\mu^-$, the amplitude is proportional to

$$\begin{aligned} A(s \to d) &\propto V_{ud}^* V_{us} f(x_u) + V_{cd}^* V_{cs} f(x_c) + V_{td}^* V_{ts} f(x_t) \\ &\simeq V_{cd}^* V_{cs} \big(f(x_c) - f(0)\big) + V_{td}^* V_{ts} \big(f(x_t) - f(0)\big) \\ &= V_{cd}^* V_{cs} \tilde{f}(x_c) + V_{td}^* V_{ts} \tilde{f}(x_t) \,. \end{aligned} \tag{10}$$

In this case, it is not necessarily a good approximation to neglect the charm mass because the corresponding term comes with much larger CKM matrix elements (see discussion in section 3.2).

An example of a $\Delta F = 2$ process is given by $B^0 - \bar{B}^0$ oscillations. An example diagram is shown in figure 2. Bottom number and down number change by two units: $|\Delta B| = |\Delta D| = 2$. Also in this example, we can work out the generic structure of the amplitude

$$A(B^0 \leftrightarrow \bar{B}^0) \propto G_F \frac{g^2}{16\pi^2} \sum_{i=u,c,t} \sum_{j=u,c,t} (V_{id}^* V_{ib})(V_{jd}^* V_{jb}) F(x_i, x_j) \,, \tag{11}$$

Where $F(x_i, x_j) = F(x_j, x_i)$ is a loop function that depends on the masses of the up-type quarks running in the loop. Using CKM unitarity and neglecting the charm and up quark masses (which is a good approximation in the case of B mixing), one finds

$$A(B^0 \leftrightarrow \bar{B}^0) \propto (V_{td}^* V_{tb})^2 \Big(F(x_t, x_t) + F(0,0) - 2F(x_t, 0)\Big) = (V_{td}^* V_{tb})^2 \tilde{F}(x_t) \,, \tag{12}$$

which highlights again the role the top mass plays in GIM breaking. It is a useful exercise to work out the corresponding expression for $K^0 - \bar{K}^0$ mixing, where one cannot neglect the charm quark mass.

2.3 Comment on Parameter Counting

In equation (5), we introduced the three Yukawa matrices that encode all information about flavor in the Standard Model. All fermion masses and the CKM matrix are determined by the Yukawa matrices. This raises the question of how many physical flavor parameters there are, and how one can determine that number.

The general rule for parameter counting says that the number of physical parameters equals the total number of parameters minus the number of symmetry generators that get broken if the parameters are non-zero [29]. More concretely, let us look at two examples to better understand how this counting works.

Example 1: Lepton Sector. In the lepton sector, we are dealing with a complex 3×3 lepton Yukawa matrix. The total number of parameters that are introduced is thus $3 \times 3 \times 2 = 18$. We can either think of it as 9 real parts and 9 imaginary parts or, more conveniently, as 9 absolute values and 9 phases.

The lepton Yukawa couplings break part of the Standard Model flavor symmetry. In particular, as the three charged leptons have all different masses, the only remaining symmetries are $U(1)$ factors of the individual lepton flavors

$$U(3)_L \times U(3)_E \to U(1)_e \times U(1)_\mu \times U(1)_\tau \ . \tag{13}$$

Now we count symmetry generators: $U(3)$ has 9 generators, 3 corresponding to mixing angles, 6 to phases; $U(1)$ has a single generator, corresponding to a phase. This means that $2 \times 9 - 3 = 15$ symmetry generators are broken. Now we use the counting rule from above and find that one has $18 - 15 = 3$ physical parameters. These can be identified with the 3 lepton masses m_e, m_μ, m_τ.

Example 2: Quark Sector. In the quark sector, we are starting with two complex 3×3 matrices, the up quark and the down quark Yukawas. This corresponds to a total number of $3 \times 3 \times 2 \times 2 = 36$ free parameters, 18 absolute values and 18 phases.

The quark Yukawas break the quark flavor symmetry almost entirely. The only remaining symmetry is baryon number

$$U(3)_Q \times U(3)_U \times U(3)_D \to U(1)_B \ . \tag{14}$$

Out of the $3 \times 9 = 27$ generators of the $U(3)^3$, all but one are broken. This means we are left with $36 - 26 = 10$ physical parameters. These correspond to the 3 up-quark masses, the 3 down-quark masses, and the 4 CKM parameters.

2.4 Flavor Spurions in the Standard Model

As discussed in the previous subsections, the Yukawa couplings break the Standard Model flavor symmetry G_{flavor}. It can be useful to keep track of this flavor breaking by promoting the Yukawa couplings to "spurions". This means we formally restore the invariance under G_{flavor} by assigning the Yukawa couplings appropriate transformation properties. In the following, we will focus on the $SU(3)^5$ part of the G_{flavor} flavor symmetry.

To make the Standard Model Lagrangian invariant under the $SU(3)^5$ flavor transformations, we promote the Yukawa couplings to bi-triplets

$$Y_u = 3_Q \times \bar{3}_U \ , \quad Y_d = 3_Q \times \bar{3}_D \ , \quad Y_e = 3_L \times \bar{3}_E \ . \tag{15}$$

In this notation, 3_Q refers to a triplet of $SU(3)_Q$, $\bar{3}_U$ to an anti-triplet of $SU(3)_U$, etc. With these transformation properties, the Yukawa Lagrangian is in fact invariant under the $SU(3)^5$, which is easily seen recalling the expression from equation (5) using a matrix notation in flavor space

$$\mathcal{L}_{\text{Yuk}} = -\bar{Q} Y_u U \tilde{H} - \bar{Q} Y_d D H - \bar{L} Y_e E H \ + \ \text{h.c.} \ . \tag{16}$$

The assigned transformation properties of the Yukawa couplings allow us to determine how the Yukawa couplings have to appear in flavor-changing amplitudes.

As an example, let us again consider the B decay from above, $B_s \to \mu^+\mu^-$. At the quark level, this corresponds to a transition from a bottom quark to a strange quark, $b \to s$. There are various currents with different chirality structures that can mediate the transition we are interested in

$$\bar{s}_L \gamma^\mu b_L \,, \quad \bar{s}_R \gamma^\mu b_R \,, \quad \bar{s}_L b_R \,, \quad \bar{s}_R b_L \,. \tag{17}$$

With the Yukawa couplings transforming as in equation (15), the Standard Model Lagrangian is invariant under $SU(3)^5$ and therefore also the $b \to s$ amplitude has to be formally invariant in the Standard Model. Based on the flavor transformation properties of the involved quarks, we can identify the minimal set of Yukawa interactions that have to appear in the amplitude. Let's go through the four currents in equation (17) one by one.

- The quarks in $\bar{s}_L \gamma^\mu b_L$ originate both from a left-handed quark doublet Q. The Q transforms as a triplet of $SU(3)_Q$. Therefore, removing the quark fields, the corresponding amplitude has to transform either as a singlet or as an octet of $SU(3)_Q$ in order to combine into a singlet with the two Q's. If the amplitude is a flavor singlet, it does not contain any flavor-violating transitions, leaving the octet as the only viable option. Constructing an $SU(3)_Q$ octet requires at least two Yukawa couplings. The simplest options are $Y_u Y_u^\dagger$ and $Y_d Y_d^\dagger$. Next, we need to project out the bottom and strange quark mass eigenstates

$$Y_d Y_d^\dagger \xrightarrow[\text{eigenstate basis}]{\text{go to mass}} \left[(Y_d^{\text{diag}})^2\right]_{23} = 0 \,, \tag{18}$$

$$Y_u Y_u^\dagger \xrightarrow[\text{eigenstate basis}]{\text{go to mass}} \left[V_{\text{CKM}}^\dagger (Y_u^{\text{diag}})^2 V_{\text{CKM}}\right]_{23} \simeq V_{tb} V_{ts}^* y_t^2 \,. \tag{19}$$

  We learn that the term $Y_d Y_d^\dagger$ does not give any flavor change in the down quark sector, as it is diagonal in the mass basis. However, because of the CKM matrix, $Y_u Y_u^\dagger$ does provide a source of down quark flavor violation. The CKM matrix elements correspond precisely to the combination that we found in section 2.2 when we looked at the Feynman diagrams for the $B_s \to \mu^+\mu^-$ decay. The proportionality to the top Yukawa coupling squared y_t^2 is a reflection of the GIM mechanism and the GIM breaking by the large top mass.

- Moving on to $\bar{s}_R \gamma^\mu b_R$, we now have two right-handed quarks that originate both from a D and, following a line of argument analogous to the one in the previous item, the corresponding amplitude needs to be a $SU(3)_D$ octet. The most economical way to construct a $SU(3)_D$ octet out of the quark Yukawa couplings is $Y_d^\dagger Y_d$, which, however, does not lead to flavor change in the down sector. The first non-trivial term that does give flavor change is

$$Y_d^\dagger Y_u Y_u^\dagger Y_d \xrightarrow[\text{eigenstate basis}]{\text{go to mass}} \left[Y_d^{\text{diag}} V_{\text{CKM}}^\dagger (Y_u^{\text{diag}})^2 V_{\text{CKM}} Y_d^{\text{diag}}\right]_{23} \simeq V_{tb} V_{ts}^* y_s y_b y_t^2 \,. \tag{20}$$

  As the bottom and strange Yukawa couplings are much smaller than 1, the contribution from such a current is highly suppressed in the Standard Model.

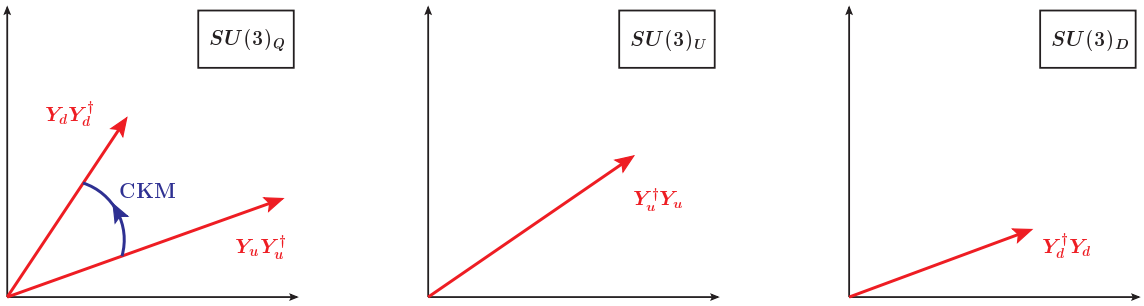

Figure 3: Illustration of the flavor octet spurions $Y_u^\dagger Y_u$, $Y_d^\dagger Y_d$, $Y_u Y_u^\dagger$, and $Y_d Y_d^\dagger$.

- The amplitudes corresponding to the scalar currents $\bar{s}_L b_R$ and $\bar{s}_R b_L$ have to transform as $\bar{3}_Q \times 3_D$ and $\bar{3}_D \times 3_Q$, respectively and therefore have to contain an odd number of Yukawa couplings. The leading terms that give flavor violation are

$$Y_u Y_u^\dagger Y_d \xrightarrow[\text{eigenstate basis}]{\text{go to mass}} \left[V_{\text{CKM}}^\dagger (Y_u^{\text{diag}})^2 V_{\text{CKM}} Y_d^{\text{diag}}\right]_{23} \simeq V_{tb} V_{ts}^* y_b y_t^2 \,, \tag{21}$$

$$Y_d^\dagger Y_u Y_u^\dagger \xrightarrow[\text{eigenstate basis}]{\text{go to mass}} \left[Y_d^{\text{diag}} V_{\text{CKM}}^\dagger (Y_u^{\text{diag}})^2 V_{\text{CKM}}\right]_{23} \simeq V_{tb} V_{ts}^* y_s y_t^2 \,. \tag{22}$$

  The amplitude involving the right-handed bottom (strange) quark is necessarily proportional to the bottom (strange) Yukawa coupling and thus suppressed compared to the $\bar{s}_L \gamma^\mu b_L$ amplitude.

The features we have seen in the $b \to s$ example above are generic in the Standard Model. The leading contributions to flavor-changing processes in the down sector involve left-handed currents. Flavor-changing currents involving right-handed down quark fields are strongly suppressed by small down quark Yukawa couplings.

Similarly, one finds that flavor-changing currents in the up sector necessarily involve down quark Yukawas and are therefore strongly suppressed in the Standard Model.

Combinations of Yukawa couplings like $Y_u^\dagger Y_u$, $Y_d^\dagger Y_d$, $Y_u Y_u^\dagger$, and $Y_d Y_d^\dagger$ define directions in flavor space. Symbolically, this is illustrated in figure 3. $Y_u^\dagger Y_u$ and $Y_d^\dagger Y_d$ live in their own $SU(3)_U$ octet space and $SU(3)_D$ octet space, respectively. $Y_u Y_u^\dagger$ and $Y_d Y_d^\dagger$ live in a common $SU(3)_Q$ octet space. The absolute orientations of these Yukawa coupling combinations are not observable. Their "length" (which can be thought of as an analogy to the eigenvalues of the Yukawa couplings and thus the fermion masses) are however observable. Furthermore, the relative orientation of $Y_u Y_u^\dagger$ and $Y_d Y_d^\dagger$ in $SU(3)_Q$ space is also observable and corresponds to the CKM matrix.

2.5 Flavor Beyond the Standard Model

Having gained a basic understanding of flavor in the context of the Standard Model, we now move on to new physics scenarios. A popular approach is to treat the Standard Model as the leading term in an effective field theory and thus extend the Standard Model by higher dimensional operators. Alternatively (or simultaneously), one can add new light degrees of freedom and consider their couplings to the Standard Model particles both at the renormalizable level and non-renormalizable

level. Generically one has

$$\mathcal{L} = \mathcal{L}_{\rm SM} + \frac{1}{\Lambda}\sum_i C_i^{(5)} Q_i^{(5)} + \frac{1}{\Lambda^2}\sum_i C_i^{(6)} Q_i^{(6)} + \ \ldots \ + \text{ new light degrees of freedom} . \tag{23}$$

The $Q_i^{(n)}$ are operators built from Standard Model fields of mass dimension $n > 4$, and the $C_i^{(n)}$ are the corresponding Wilson coefficients. The higher dimensional operators with larger mass dimensions are suppressed by higher and higher powers of the inverse of a new physics scale Λ. Under the assumption that the full Standard Model gauge group $SU(3)_c \times SU(2)_L \times U(1)_Y$ is realized linearly, the extension of the Standard Model by the tower of higher dimensional operators is referred to as the Standard Model Effective Field Theory (SMEFT) [39].

The higher dimensional operators that contain quark or lepton fields, as well as the couplings of the new particles to quarks and leptons constitute, in general, new sources of flavor violation. In many cases, the new sources of flavor violation are strongly constrained by existing measurements of flavor transitions. The most important examples that illustrate the strong constraints that can be derived from flavor transitions are meson anti-meson oscillations.

There are four neutral meson systems in which particle anti-particle oscillations can occur: $K^0 - \bar{K}^0$ oscillations corresponding to a $s \leftrightarrow d$ transition, $B^0 - \bar{B}^0$ oscillations corresponding to a $b \leftrightarrow d$ transition, $B_s - \bar{B}_s$ oscillations corresponding to a $b \leftrightarrow s$ transition, and $D^0 - \bar{D}^0$ oscillations corresponding to a $c \leftrightarrow u$ transition.

In each case, the oscillations can be mediated by eight independent dimension-6 four-fermion operators that are invariant under the unbroken Standard Model gauge symmetry $SU(3)_c \times U(1)_{\rm em}$. In the example of kaon oscillations, the operators are (see e.g. [40])

$$Q^{VLL} = (\bar{s}\gamma_\mu P_L d)(\bar{s}\gamma^\mu P_L d) , \qquad Q^{VRR} = (\bar{s}\gamma_\mu P_R d)(\bar{s}\gamma^\mu P_R d) , \tag{24}$$

$$Q_1^{LR} = (\bar{s}\gamma_\mu P_L d)(\bar{s}\gamma^\mu P_R d) , \tag{25}$$

$$Q_2^{LR} = (\bar{s} P_L d)(\bar{s} P_R d) , \tag{26}$$

$$Q_1^{SLL} = (\bar{s} P_L d)(\bar{s} P_L d) , \qquad Q_1^{SRR} = (\bar{s} P_R d)(\bar{s} P_R d) , \tag{27}$$

$$Q_2^{SLL} = (\bar{s}\sigma_{\mu\nu} P_L d)(\bar{s}\sigma^{\mu\nu} P_L d) , \qquad Q_2^{SRR} = (\bar{s}\sigma_{\mu\nu} P_R d)(\bar{s}\sigma^{\mu\nu} P_R d) . \tag{28}$$

For the other meson systems, the operators can be defined analogously with appropriate replacements of the quark fields. There are several equivalent $\Delta F = 2$ operator bases. Another one that is often used is (see e.g. [41])

$$Q_1 = (\bar{s}_\alpha \gamma_\mu P_L d_\alpha)(\bar{s}_\beta \gamma^\mu P_L d_\beta) , \qquad Q_1' = (\bar{s}_\alpha \gamma_\mu P_R d_\alpha)(\bar{s}_\beta \gamma^\mu P_R d_\beta) , \tag{29}$$

$$Q_2 = (\bar{s}_\alpha P_L d_\alpha)(\bar{s}_\beta P_L d_\beta) , \qquad Q_2' = (\bar{s}_\alpha P_R d_\alpha)(\bar{s}_\beta P_R d_\beta) , \tag{30}$$

$$Q_3 = (\bar{s}_\alpha P_L d_\beta)(\bar{s}_\beta P_L d_\alpha) , \qquad Q_3' = (\bar{s}_\beta P_R d_\alpha)(\bar{s}_\beta P_R d_\alpha) , \tag{31}$$

$$Q_4 = (\bar{s}_\alpha P_L d_\alpha)(\bar{s}_\beta P_R d_\beta) , \tag{32}$$

$$Q_5 = (\bar{s}_\alpha P_L d_\beta)(\bar{s}_\beta P_R d_\alpha) , \tag{33}$$

where α, β are quark color indices. Using Fierz transformations on the operators Q_3, Q_3', and Q_5, one can show the equivalence of the two operator bases.

Adding the contributions of the above operators to the Standard Model contributions to meson mixing observables and comparing the results to the corresponding experimental measurements,

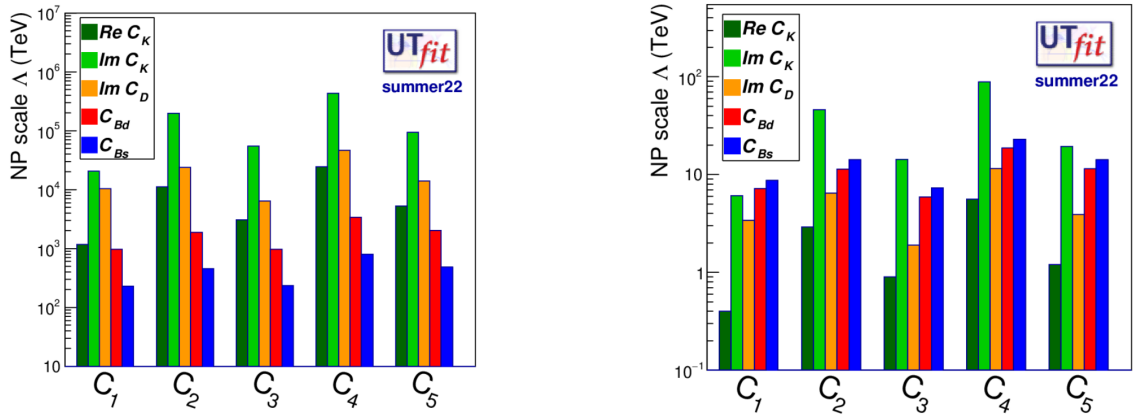

Figure 4: Constraints on the new physics scale Λ from meson mixing. One dimension-6 $\Delta F = 2$ operator is switched on at a time. In the left-hand plot, the absolute value of the non-zero Wilson coefficient is set to 1. In the right-hand plot, the absolute value of the non-zero Wilson coefficient is set to the CKM matrix combination that governs the flavor transition in the Standard Model. (Plots taken from [42].)

one can derive constraints on the Wilson coefficients and the new physics scale. The result of this exercise is shown in the plots of figure 4. On the left-hand side, the Wilson coefficients are set to 1 one at a time and the constraint on the new physics scale is shown by the bars for the various meson systems. The constraint for $C'_{1,2,3}$ are identical to the ones for $C_{1,2,3}$ and therefore not shown. We see that in some cases, very high new physics scales as large as few 10^5 TeV are probed!

It is conceivable that the new physics Wilson coefficients are not of $O(1)$ but instead suppressed by small new physics flavor mixing angles, similar to the Standard Model CKM mixing angles. On the right-hand side, the absolute value of the Wilson coefficients is set to the corresponding CKM matrix elements in the Standard Model, i.e. $|C_i| = |V_{ts}^* V_{td}|^2, |V_{td}^* V_{tb}|^2, |V_{ts}^* V_{tb}|^2, |V_{ub}^* V_{cb}|^2$ for kaon mixing, B^0 mixing, B_s mixing, and D^0 mixing, respectively. In such a case, the constraints on the new physics scale are much weaker but can still reach several 10's of TeV.

The high sensitivity of meson mixing to flavor-changing new physics originates from the strong suppression of $\Delta F = 2$ flavor-changing neutral currents in the Standard Model. Generically speaking, the new physics contribution competes with a weak Standard Model amplitude that is loop-suppressed and CKM-suppressed. E.g. for kaon mixing

$$\frac{C_i}{\Lambda^2} \qquad \text{vs.} \qquad G_F \frac{g^2}{16\pi^2} |V_{ts}^* V_{td}|^2 \,. \tag{34}$$

Allowing for an $O(1)$ new physics contribution to kaon mixing can give sensitivities to new physics far above the weak scale $1/\sqrt{G_f} \propto v = 246$ GeV.

Interestingly, not all $\Delta F = 2$ operators listed above are invariant under the full Standard Model gauge symmetry $SU(3)_c \times SU(2)_L \times U(1)_Y$. This means that not all of them show up in the SMEFT at mass dimension 6. Can you identify them? Can you construct dimension-8 operators that map onto them below the electroweak scale? What does this imply for the bounds shown in figure 4?

The four-fermion operators that are constrained by meson mixing might arise from integrating out heavy new physics particles that have flavor-changing couplings. One simple example would be a new vector boson X that couples in a flavor-violating way to right-handed strange and down

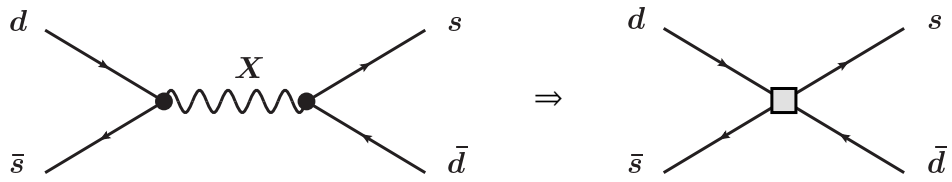

Figure 5: Example of a new physics contribution to kaon mixing from a new physics vector boson X with flavor-changing couplings.

quarks. At low energies, the effect of this new particle would appear as a contribution to the Wilson coefficient of the operator $Q^{VRR} = Q_2$, as sketched in figure 5.

$$g^R_{sd}(\bar{s}\gamma_\mu P_R d)X^\mu \qquad \Rightarrow \qquad \frac{(g^R_{sd})^2}{2m_X^2}(\bar{s}\gamma_\mu P_R d)(\bar{s}\gamma^\mu P_R d)\,. \tag{35}$$

(It is a good exercise to verify the factor 1/2 in the Wilson coefficient.) Such a spin-1 particle with flavor-changing couplings can for example arise in models with spontaneously broken generation-dependent gauge symmetries. Other classic examples of new physics scenarios that are strongly constrained by meson mixing include Supersymmetric models where loops of squarks and gluinos contribute to meson mixing (see e.g. [43, 44]), and models with warped extra dimensions in which tree-level exchanges of Kaluza Klein gluons contribute (see e.g. [45, 46]).

2.6 Strategies to Avoid Flavor Constraints

As we have seen in the previous subsection, flavor-changing processes, meson mixing in particular, are very sensitive to new sources of flavor violation. If new physics comes with large flavor mixing, the new physics scale is often constrained to be many orders of magnitude above the electroweak scale.

While the LHC has so far not found any evidence for new physics particles, arguments based on the naturalness of the electroweak scale still generically suggest that new physics degrees of freedom should exist not far above the regime explored by the LHC. If such new physics indeed exists, why have we not seen it yet indirectly in flavor observables? This question is sometimes referred to as the new physics flavor puzzle.

In general, one can consider three basic strategies to suppress new physics contributions to flavor-changing processes:

(1) Make the new physics scale Λ very large. This corresponds to a *decoupling* of the new physics effects but (at least naively) clashes with the naturalness arguments.

(2) Assume that the new physics couplings have a *trivial flavor structure*. That means the new couplings do not constitute sources of flavor violation. They are unit matrices in flavor space and thus flavor conserving in any flavor basis. Note that this does not necessarily mean that there are no new physics contributions to flavor-changing processes. It simply means that new physics contributions have to come with the same CKM suppression as the Standard Model contributions.

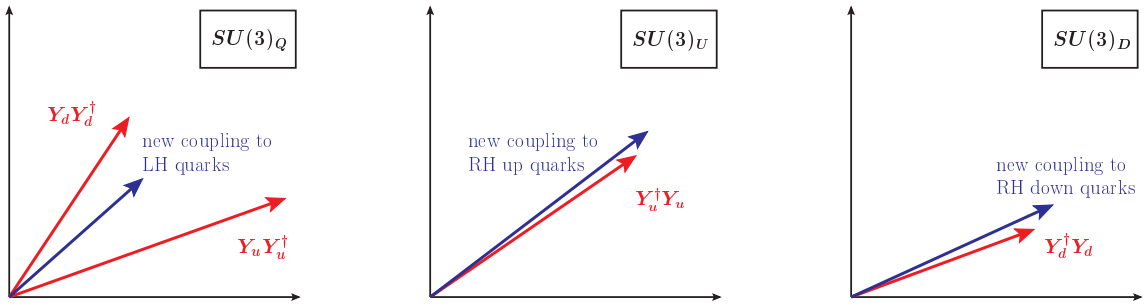

Figure 6: Illustration of new flavor changing couplings and their relation to the Standard Model flavor spurions $Y_u^\dagger Y_u$, $Y_d^\dagger Y_d$, $Y_u Y_u^\dagger$, and $Y_d Y_d^\dagger$.

(3) Assume that the new couplings approximately "point in the same flavor direction" as the Yukawa couplings. This is known as *flavor alignment* [47]. As only relative flavor directions are observable, flavor mixing is small in these models.

One can consider two sub-classes of flavor alignment:

(3a) One assumes that the new flavor-violating couplings are proportional to the Standard Model Yukawa couplings (or suitable powers of Yukawa couplings) such that one formally retains invariance under the Standard Model flavor symmetry in the spurion picture. This framework is known as *Minimal Flavor Violation* [48]. In Minimal Flavor Violation, all quark flavor transitions are governed by the CKM matrix as in the Standard Model.

(3b) In a less restrictive framework, one allows new flavor-violating couplings as long as they are approximately diagonal in the fermion mass eigenstate basis. This is illustrated in the diagrams of figure 6. In the $SU(3)_U$ and $SU(3)_D$ spaces, the alignment with the Standard Model Yukawas can in principle be exact, i.e. the Yukawa couplings and the new physics couplings can be diagonalized simultaneously. In the $SU(3)_Q$ space that corresponds to the left-handed quarks, exact alignment can be achieved for either up-quarks or down-quarks, but not both at the same time. Therefore, such scenarios typically have to face stringent constraints from either down-type FCNCs or up-type FCNCs (or both).

3. Determination of the Standard Model Flavor Parameters

In subsection 3.1 we will briefly summarize the status of measurements of the charged lepton and the quark masses. In subsection 3.2 we review the determination of the CKM matrix elements.

3.1 Quark and Lepton Masses

The masses of the charged leptons are known with remarkable precision. In particular, combining information from Hydrogen spectroscopy and the precession and cyclotron motion of the electron, one finds the mass of the electron with a relative precision of 3×10^{-10} [49]

$$m_e = 510.99895000(15)\ \text{keV}\ . \tag{36}$$

The most precise determination of the muon mass comes from the hyperfine splitting of muonium and has a relative uncertainty of 2×10^{-8} [49]

$$m_\mu = 105.6583755(23)\ \text{MeV}\ . \tag{37}$$

The tau mass has a substantially larger uncertainty. The PDG average reads [50]

$$m_\tau = 1.77686(12)\ \text{GeV}\ , \tag{38}$$

and is dominated by results from a $\tau^+\tau^-$ threshold scan at BESIII [51]. The quoted lepton masses are all pole masses.

Moving on to the quarks, we note that quarks are not observed as physical particles but (with the exception of the top quark) are confined in hadrons. Measurements of quark masses are therefore indirect, and one needs to carefully specify a scheme when one quotes quark masses. The masses of the light quarks u, d, s can be determined from lattice simulations of meson and baryon masses that depend on the quark masses. The results are quoted as $\overline{\text{MS}}$ masses at a renormalization scale of $\mu = 2$ GeV [50]

$$m_u = \bar{m}_u(2\ \text{GeV}) = 2.16^{+0.49}_{-0.26}\ \text{MeV}\ , \tag{39}$$

$$m_d = \bar{m}_d(2\ \text{GeV}) = 4.67^{+0.48}_{-0.17}\ \text{MeV}\ , \tag{40}$$

$$m_s = \bar{m}_s(2\ \text{GeV}) = 93.4^{+8.6}_{-3.4}\ \text{MeV}\ . \tag{41}$$

For the charm and bottom masses, one can make use of the fact that their masses are larger than the QCD scale and employ effective theories. Both lattice and continuum calculations are used to determine the quark masses from e.g. the masses of B or D mesons, or charmonium and bottomonium masses. Also $e^+e^- \to$ hadron data close to the $b\bar{b}$ and $c\bar{c}$ thresholds is used. The PDG quotes the charm and bottom masses in the $\overline{\text{MS}}$ scheme at a renormalization scale equal to the mass itself

$$m_c = \bar{m}_c(\bar{m}_c) = 1.27(2)\ \text{GeV}\ , \tag{42}$$

$$m_b = \bar{m}_b(\bar{m}_b) = 4.18(3)\ \text{GeV}\ . \tag{43}$$

The top quark is by far the heaviest of the quarks, and its mass can be determined in a variety of ways. The most precise results are based on event kinematics in $t\bar{t}$ production at the LHC. Alternative measurements extract the top quark mass from the $t\bar{t}$ production cross-section. The advantage of the cross-section method is that it gives the top mass in a well-defined renormalization scheme. The PDG quotes the following top pole mass from cross-section measurements

$$m_t = m_t^{\text{pole}} = 172.5(7)\ \text{GeV}\ . \tag{44}$$

Figure 7 shows a summary of the masses of the quarks and charged leptons of the Standard Model. For comparison, also the masses of neutrinos, the weak gauge bosons, and the Higgs are shown. It is remarkable that the quark masses span five orders of magnitude. Between the mass of the lightest charged fermion (the electron) and the heaviest (the top quark), there are almost six orders of magnitude.

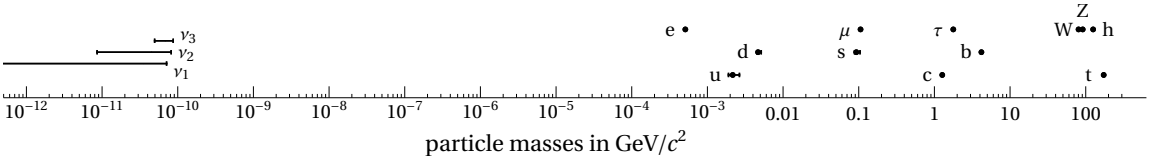

Figure 7: Masses of the Standard Model particles. The masses of the Higgs, weak gauge bosons, quarks, and charged leptons are taken from the PDG [50]. The shown neutrino mass ranges are determined from the known squared mass differences from neutrino oscillations [50] and the constraint on the sum of neutrino masses from Planck [52]. The lightest neutrino could be massless. (Plot taken from [53].)

3.2 CKM Matrix Elements

As mentioned in section 2, the CKM matrix is determined by three mixing angles and one CP violating phase that we denote with θ_{12}, θ_{13}, θ_{23}, and δ, respectively. The standard parameterization is given by a product of three rotation matrices

$$V_{\text{CKM}} = \begin{pmatrix} V_{ud} & V_{us} & V_{ub} \\ V_{cd} & V_{cs} & V_{cb} \\ V_{td} & V_{ts} & V_{tb} \end{pmatrix} = \begin{pmatrix} 1 & 0 & 0 \\ 0 & c_{23} & s_{23} \\ 0 & -s_{23} & c_{23} \end{pmatrix} \begin{pmatrix} c_{13} & 0 & s_{13}e^{-i\delta} \\ 0 & 1 & 0 \\ -s_{13}e^{i\delta} & 0 & c_{13} \end{pmatrix} \begin{pmatrix} c_{12} & s_{12} & 0 \\ -s_{12} & c_{12} & 0 \\ 0 & 0 & 1 \end{pmatrix} , \tag{45}$$

where we used the notation $c_{ij} = \cos(\theta_{ij})$ and $s_{ij} = \sin(\theta_{ij})$. In this standard parameterization, the elements V_{ud}, V_{us}, V_{cb}, and V_{tb} are real. Experimentally, one finds that the three mixing angles follow a hierarchical pattern: $1 \gg \theta_{12} \gg \theta_{23} \gg \theta_{13}$. The origin of this hierarchy remains unexplained in the Standard Model. The hierarchy in the mixing angles can be made manifest by using the so-called Wolfenstein parameterization [54], which trades the parameters θ_{12}, θ_{13}, θ_{23}, and δ for the Wolfenstein parameters λ, A, ρ, and η, which can be defined in the following way

$$s_{12} = \lambda = \frac{|V_{us}|}{\sqrt{|V_{ud}|^2 + |V_{us}|^2}} , \quad s_{23} = A\lambda^2 = \lambda \left| \frac{V_{cb}}{V_{us}} \right| , \quad s_{13}e^{i\delta} = A\lambda^3(\rho + i\eta) . \tag{46}$$

Treating λ as a small expansion parameter, one finds the approximation

$$V_{\text{CKM}} = \begin{pmatrix} 1 - \frac{\lambda^2}{2} & \lambda & A\lambda^3(\rho - i\eta) \\ -\lambda & 1 - \frac{\lambda^2}{2} & A\lambda^2 \\ A\lambda^3(1 - \rho - i\eta) & -A\lambda^2 & 1 \end{pmatrix} + \mathcal{O}(\lambda^4) . \tag{47}$$

Higher orders in the expansion can be easily obtained by inserting the relations from equation (46) into equation (45) and expanding in the parameter λ. It is a good exercise to determine the λ^4 terms.

The unitarity of the CKM matrix implies relations among its elements. In particular, one has

$$\sum_i V_{ij}V_{ik}^* = \delta_{jk} , \quad \sum_j V_{ij}V_{kj}^* = \delta_{ik} . \tag{48}$$

The six independently vanishing combinations of CKM elements can be represented by so-called "unitarity triangles", corresponding to three complex numbers adding up to zero. The most important of these triangles (one of those that have all sides of the same order) is the following:

$$V_{ud}V_{ub}^* + V_{cd}V_{cb}^* + V_{td}V_{tb}^* = 0 \quad \Leftrightarrow \quad \frac{V_{ud}V_{ub}^*}{V_{cd}V_{cb}^*} + 1 + \frac{V_{td}V_{tb}^*}{V_{cd}V_{cb}^*} = 0 . \tag{49}$$

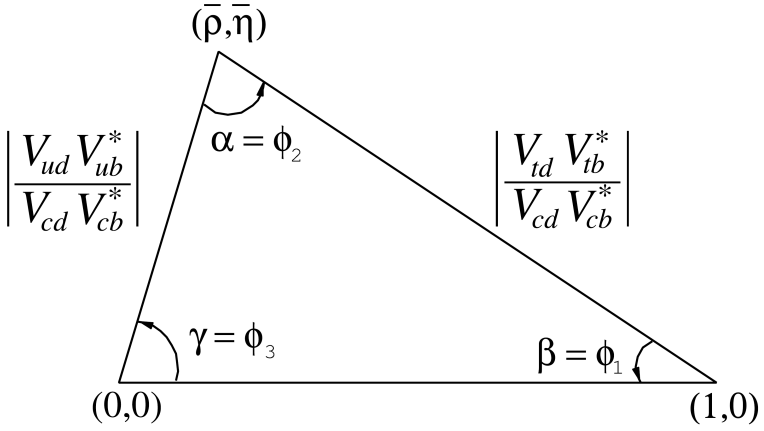

Figure 8: A sketch of the unitarity triangle. (Plot taken from [50].)

The version of this triangle in which one side is normalized to 1 is usually referred to as "the" unitarity triangle and it is illustrated in figure 8. The apex of this triangle is given by the parameters $\bar\rho$ and $\bar\eta$ that can be defined by

$$\bar\rho + i\bar\eta = -\frac{V_{ud}V_{ub}^*}{V_{cd}V_{cb}^*} \,. \tag{50}$$

Up to small corrections, $\bar\rho$ and $\bar\eta$ coincide with the Wolfenstein parameters ρ and η introduced above

$$\bar\rho = \rho\left(1-\frac{\lambda^2}{2}+...\right), \quad \bar\eta = \eta\left(1-\frac{\lambda^2}{2}+...\right) \,. \tag{51}$$

The three angles in the unitarity triangle are given by

$$\beta=\phi_1=\arg\left(-\frac{V_{cd}V_{cb}^*}{V_{td}V_{tb}^*}\right), \quad \alpha=\phi_2=\arg\left(-\frac{V_{td}V_{tb}^*}{V_{ud}V_{ub}^*}\right), \quad \gamma=\phi_3=\arg\left(-\frac{V_{ud}V_{ub}^*}{V_{cd}V_{cb}^*}\right) \,. \tag{52}$$

Measurements of CKM matrix elements are often projected into the $\bar\rho$-$\bar\eta$ plane, providing a convenient way to compare different measurements and to check that they give consistent results.

Next, we give a very brief summary of the most important ways to determine the absolute values of the various CKM matrix elements.

The most precise determination of $|V_{ud}|$ comes from superallowed nuclear β decay [50]

$$|V_{ud}| = 0.973737(31) \,. \tag{53}$$

The uncertainty is dominated by nuclear structure effects. Alternatively, also the neutron lifetime or pion beta decay $\pi^+ \to \pi^0 e^+ \nu$ can be used to determine $|V_{ud}|$, albeit currently with larger experimental uncertainties. The pion decay experiment PIONEER aims at a precision measurement of $\pi^+ \to \pi^0 e^+ \nu$, providing a determination of $|V_{ud}|$ that is expected to rival the precision of the nuclear beta decays [55].

The CKM matrix element $|V_{us}|$ is extracted from semi-leptonic kaon decays $K \to \pi \ell \nu$, where $\ell = e, \mu$. Combining measurements of the kaon decay rates and lattice results for the $K \to \pi$ form factor one finds [50]

$$|V_{us}| = 0.2231(6) \,. \tag{54}$$

The ratio $|V_{us}/V_{ud}|$ can be determined with comparable precision from the ratio of leptonic kaon and pion decays, $K \to \mu\nu$ vs. $\pi \to \mu\nu$. Interestingly, the determinations of $|V_{ud}|$, $|V_{us}|$, and $|V_{us}/V_{ud}|$ are in slight tension with the unitarity of the CKM matrix that demands $|V_{ud}|^2 + |V_{us}|^2 = 1 - |V_{ub}|^2 \simeq 1$, where the $|V_{ub}|^2$ term is tiny (see equation (58) below) and can be safely neglected. This tension is at the level of $\sim 3\sigma$ and is known as the "Cabibbo angle anomaly" [56, 57].

The best direct determination of the elements $|V_{cd}|$ and $|V_{cs}|$ comes from leptonic or semi-leptonic D meson decays, like $D \to \mu\nu$, $D_s \to \mu\nu$, $D \to \pi\ell\nu$, and $D \to K\ell\nu$. The current averages from the PDG are [50]

$$|V_{cd}| = 0.221(4)\,, \tag{55}$$

$$|V_{cs}| = 0.975(6)\,. \tag{56}$$

The precision of these values cannot compete with the indirect determination that makes use of the unitarity of the CKM matrix and the values of $|V_{ud}|$ and $|V_{us}|$.

The most precise direct determinations of the CKM elements $|V_{cb}|$ and $|V_{ub}|$ come from semi-leptonic decays of B mesons that are based on the $b \to c\ell\nu$ or $b \to u\ell\nu$ transition. On the one hand, there are the "inclusive" determinations based on the decays $B \to X_c\ell\nu$ and $B \to X_u\ell\nu$, where X_c and X_u refer to the sum over all hadronic states with charm or up flavor. On the other hand, there are the "exclusive" determinations that focus on particular hadronic final states like $B \to D\ell\nu$ or $B \to D^*\ell\nu$ for $|V_{cb}|$ and $B \to \pi\ell\nu$ for $|V_{ub}|$. For many years, there have been tensions between the inclusive and exclusive determinations at the level of $2\sigma - 3\sigma$. The world averages quoted by the PDG take into account these tensions by inflating the uncertainties [50]

$$|V_{cb}| = 40.8(1.4) \times 10^{-3}\,, \tag{57}$$

$$|V_{ub}| = 3.82(20) \times 10^{-3}\,. \tag{58}$$

Given the tensions between the exclusive and inclusive determinations, care has to be taken when using the above averages.

The element $|V_{tb}|$ can be directly measured in top quark decays $t \to Wb$ and in single top production at hadron colliders. Combining the existing results from the Tevatron and LHC, one finds [50]

$$|V_{tb}| = 1.014(29)\,. \tag{59}$$

Similar to $|V_{cd}|$ and $|V_{cs}|$, a much more precise value for $|V_{tb}|$ can be obtained indirectly using the unitarity of the CKM matrix.

In contrast to all the other CKM matrix elements, the best direct measurements of $|V_{ts}|$ and $|V_{td}|$ do not come from tree-level processes but from loop-level processes, B meson oscillations in particular. In fact, the dominant top loop contributions to the B^0 and B_s oscillation frequencies (see the diagram in figure 2 and the corresponding discussion in section 2.2) are proportional to $(V_{td}V_{tb}^*)^2$ and $(V_{ts}V_{tb}^*)^2$, respectively. The oscillation frequencies are measured with remarkable precision [33]. The limiting factor in extracting the values of $|V_{ts}|$ and $|V_{td}|$ are hadronic matrix elements that have to be taken from the lattice [34]. One finds

$$|V_{td}| = 8.6(2) \times 10^{-3}\,. \tag{60}$$

$$|V_{ts}| = 41.5(9) \times 10^{-3}\,. \tag{61}$$

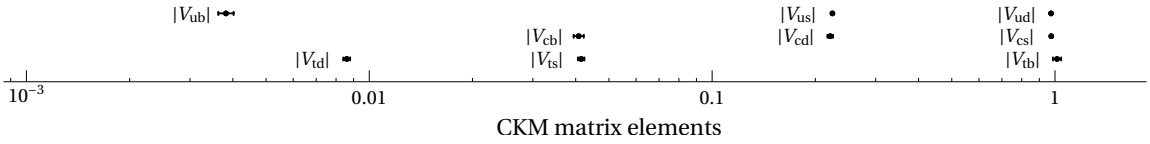

Figure 9: The absolute values of the CKM matrix elements from direct measurements. Shown are also the 1σ uncertainties.

The uncertainties of the loop level determinations of $|V_{ts}|$ and $|V_{td}|$ are comparable to those of the tree level determinations of $|V_{cb}|$ and $|V_{ub}|$. The absolute values of all the CKM matrix elements are summarized in figure 9. They span almost 3 orders of magnitude.

Having discussed the absolute values of the CKM matrix elements, we move on to the CKM phase. A non-zero phase of the CKM matrix indicates CP violation. Focusing on the part of the Standard Model Lagrangian that contains the CKM matrix and performing a CP transformation, one finds

$$\begin{aligned}\mathcal{L}_{\rm SM} \supset \frac{g}{\sqrt{2}} V_{ij} \bar{u}_i \gamma^\mu P_L d_j W^+_\mu + \frac{g}{\sqrt{2}} V^*_{ij} \bar{d}_j \gamma^\mu P_L u_i W^-_\mu \\ \xrightarrow{\text{CP transformation}} \frac{g}{\sqrt{2}} V_{ij} \bar{d}_j \gamma^\mu P_L u_i W^-_\mu + \frac{g}{\sqrt{2}} V^*_{ij} \bar{u}_i \gamma^\mu P_L d_j W^+_\mu \,. \end{aligned} \tag{62}$$

The above result implies that CP is violated unless all CKM matrix elements are real $V_{ij} \neq V^*_{ij}$. Phrased in the Wolfenstein parameterization, this corresponds to $\bar{\eta} \neq 0$ and implies a unitarity triangle with a non-zero surface. It also implies that the phase of the CKM matrix can be determined using measurements of CP-violating phenomena.

Famously, the angle β of the unitarity triangle can be measured using the time-dependent CP asymmetry in the B meson decay $B \to J/\psi K_S$

$$\frac{\text{BR}(\bar{B}^0(t) \to J/\psi K_S) - \text{BR}(B^0(t) \to J/\psi K_S)}{\text{BR}(\bar{B}^0(t) \to J/\psi K_S) - \text{BR}(B^0(t) \to J/\psi K_S)} \simeq \sin(2\beta) \sin(\Delta M_d t) \,. \tag{63}$$

The current world average that is dominated by results from BaBar, Belle, and LHCb is [33]

$$\beta = (22.2 \pm 0.7)^\circ \tag{64}$$

The angles α and γ can be determined from time-dependent CP asymmetries in $B \to \rho\rho$, $B \to \pi\pi$, $B \to \rho\pi$ and CP asymmetries in $B \to DK$ decays, respectively. The current world averages are [33]

$$\alpha = (85.2^{+4.8}_{-4.3})^\circ \,, \quad \gamma = (66.2^{+3.4}_{-3.6})^\circ \,. \tag{65}$$

Combining all the information above as well as measurements of additional observables that are sensitive to CKM matrix elements (in particular ϵ_K that is a measure of CP violation in kaon mixing), global fits of the CKM matrix can be performed. Such fits are highly overconstrained and, overall, show good consistency.

$$\lambda = 0.22500^{+0.00024}_{-0.00022} \,, \quad A = 0.8132^{+0.0119}_{-0.0060} \,, \quad \bar{\rho} = 0.1566^{+0.0085}_{-0.0048} \,, \quad \bar{\eta} = 0.3475^{+0.0118}_{-0.0054} \,, \tag{66}$$

$$\lambda = 0.22519(83) \,, \quad A = 0.828(11) \,, \quad \bar{\rho} = 0.161(10) \,, \quad \bar{\eta} = 0.347(10) \,. \tag{67}$$

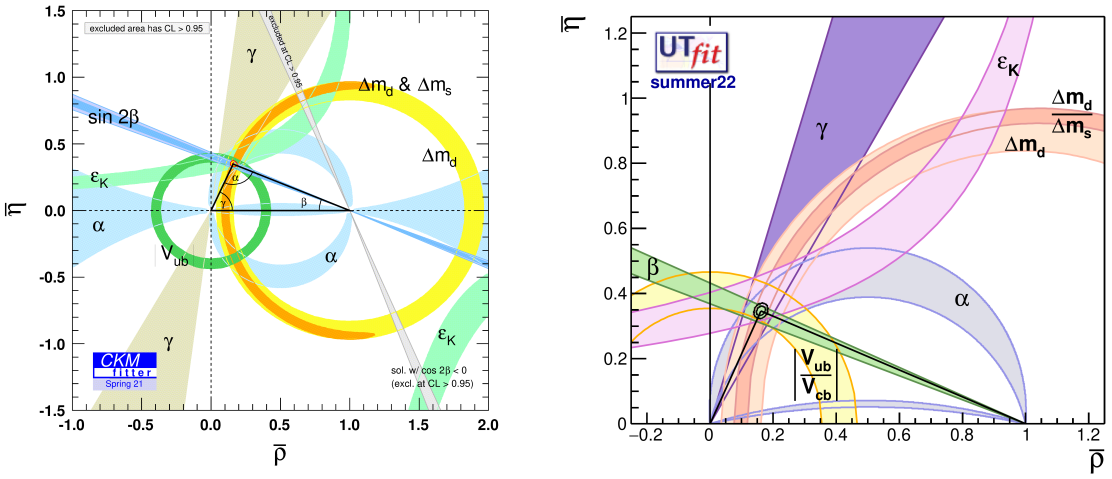

Figure 10: The unitarity triangle from the Standard Model global fit. Left: result from the CKMfitter collaboration [58]. Right: result from the UTfit collaboration [59, 60].

Above we quote the results of the CKMfitter [58] collaboration in equation (66) and the UTfit [59] collaboration in equation (67), which are in good agreement with each other The corresponding plots of the unitarity triangle are given in figure 10. All measurements overlap consistently in the $\bar{\rho} - \bar{\eta}$ plane.

4. The Standard Model Flavor Puzzle

As discussed in the previous section, the determination of the Standard Model flavor parameters gives a consistent picture in which all flavor-changing transitions among quarks are described by the CKM matrix. However, many questions about flavor remain still unanswered. This includes the zeroth order question, "Why are there three generations of quarks and leptons?", as well as questions about the particular values of the Standard Model flavor parameters:

- What is the origin of the hierarchical spectrum of quarks and charged leptons?
- What is the origin of the hierarchical mixing angles in the CKM matrix?

These questions are usually referred to as the *Standard Model flavor puzzle*. We should note that there is nothing inconsistent about flavor in the Standard Model. Moreover, the observed hierarchies are technically natural, i.e. stable under radiative corrections. Nevertheless, the hierarchical patterns of masses and CKM mixing elements shown in figures 7 and 9 are suggestive of some underlying physics and call for an explanation.

4.1 Generating Flavor Hierarchies

In order to address the Standard Model flavor puzzle, one first needs to make assumptions about electroweak symmetry breaking. There are two options:

(1) Electroweak symmetry breaking is as in the Standard Model, i.e. the only source of electroweak symmetry breaking is the vacuum expectation value of the Higgs boson. In this case, the hierarchies in the fermion masses and the quark mixing angles need to be explained by hierarchies in the Yukawa couplings. The task is then to introduce mechanisms that generate hierarchies in Yukawa couplings.

One issue that one has to face in this context is that Yukawa couplings are marginal interactions. This means that the physics that determines their structure could be arbitrarily heavy. Models that try to explain hierarchical Yukawa couplings are thus not necessarily testable unless part of the models' new physics spectrum is sufficiently light to give experimentally observable signatures.

(2) There is an extended electroweak symmetry breaking sector, with multiple sources of electroweak symmetry breaking. In this case, the hierarchies in masses and mixing angles could be due to hierarchies in the sources of electroweak symmetry breaking. The simplest example is a 2 Higgs Doublet Model (2HDM) in which the 2 Higgses have very different vacuum expectation values. This can happen, for example, in the Minimal Supersymmetric Standard Model (MSSM) and is referred to as the "large $\tan\beta$ regime" of the MSSM, where $\tan\beta = v_2/v_1$ is the ratio of the two vacuum expectation values. At tree level, the MSSM is a 2HDM of type 2, which means that one Higgs couples to up-type quarks, while the second Higgs couples to down-type quarks and charged leptons. For $\tan\beta \simeq 50$ one has top, bottom, and tau Yukwa couplings approximately of the same order $y_t \sim y_b \sim y_\tau \sim O(1)$. The remaining hierarchies in the fermion masses and the CKM matrix, however, still require an explanation in terms of partly hierarchical Yukawa couplings.

This is a fairly generic feature. Large hierarchies (larger than $\sim 16\pi^2 \sim 10^2$) in scalar vevs are not radiatively stable. Therefore, in models with extended electroweak symmetry breaking sectors, one generically still needs to explain some of the flavor hierarchies with hierarchies in Yukawa couplings as in case (1).

In the following, we briefly discuss various ways to generate hierarchical Yukawa couplings. A more detailed discussion can be found, for example, in [53]. Many ideas have been put forward to explain hierarchical Yukawa couplings using new UV dynamics. The list includes:

(a) Models with spontaneously broken flavor symmetries, with the most famous example the so-called Froggatt-Nielsen models [61] that are based on a $U(1)$ flavor symmetry.

(b) Models with extra dimensions in which small Yukawa couplings are the result of exponentially small wave function overlap in the extra dimension between the light fermions and the Higgs [62–64].

(c) Models of partial compositeness, in which the Standard Model fermions mix with heavy resonances of a strongly interacting sector. The light Standard Model fermions are mainly elementary, while the heavy ones have a sizable composite component [65].

(d) Models of radiative flavor, where small masses are absent at the tree level but arise at the loop level [66].

4.2 A Simple Froggatt-Nielsen Model

Here, we discuss a simple example of a setup with a spontaneously broken $U(1)$ flavor symmetry that gives an up-quark mass much smaller than the top-quark mass. The starting point is to introduce an abelian flavor symmetry $U(1)_{\rm FN}$ and to assign each Standard Model fermion a charge. Let's assume that both the left-handed and the right-handed top quarks are uncharged, while the left-handed and the right-handed up quarks have a moderately large charge of ± 3. We will also assume that the Higgs boson is uncharged under the flavor symmetry:

$$Q(H) = 0\,, \quad Q(t_L) = 0\,, \quad Q(t_R) = 0\,, \quad Q(u_L) = +3\,, \quad Q(u_R) = -3\,. \tag{68}$$

With these charge assignments, the Yukawa coupling of the top quark is trivially compatible with the flavor symmetry, because $Q(t_R) - Q(t_L) - Q(H) = 0$ and we can introduce the coupling

$$\mathcal{L} \supset Y_t \bar{t}_L t_R \tilde{H} \; + \; \text{h.c.}\,. \tag{69}$$

The top Yukawa coupling is thus generically expected to be $O(1)$. The Yukawa coupling of the up quark, on the other hand, is forbidden by the flavor symmetry, as $Q(u_R) - Q(u_L) - Q(H) = -6 \neq 0$.

In order for the up-quark to couple to the Higgs, we introduce an additional scalar field Φ, usually referred to as a *flavon*, that has Froggatt-Nielsen charge $Q(\Phi) = 1$ and is a Standard Model singlet. We will assume that this scalar acquires a vacuum expectation value $\Phi \to \langle\Phi\rangle$ and thus spontaneously breaks the $U(1)_{\rm FN}$ flavor symmetry. In such a setup, we can have a higher dimensional operator that provides an effective up quark Yukawa coupling Y_u after the breaking of the $U(1)_{\rm FN}$ symmetry. In the chosen example, it is a dimension 10 operator containing six powers of the flavon to compensate the flavor charges of the up quark

$$\mathcal{L} \supset \tilde{Y}_u \left(\frac{\Phi}{\Lambda}\right)^6 \bar{u}_L u_R \tilde{H} \; + \; \text{h.c.} \;\; \to \;\; Y_u \bar{u}_L u_R \tilde{H} \; + \; \text{h.c.} \quad \text{with } Y_u = \tilde{Y}_u \left(\frac{\langle\Phi\rangle}{\Lambda}\right)^6 . \tag{70}$$

Here, $\tilde{Y}_u$ is a "proto" Yukawa coupling, generically expected to be of $O(1)$ and Λ is a characteristic scale of the physics that UV-completes the higher dimensional operator. A canonical UV completion would be given by a set of heavy vectorlike quarks χ_i with Froggatt-Nielsen charges that allow them to be chained up to connect the up-quark with the Higgs, as shown in Figure 11. As long as $\langle\Phi\rangle < \Lambda$, the effective up quark Yukawa coupling Y_u is exponentially suppressed. With a typical choice of $\langle\Phi\rangle/\Lambda \simeq \lambda \simeq 0.23$, one finds $m_u/m_t \sim (\langle\Phi\rangle/\Lambda)^6 \sim 10^{-4}$, not too far from the observed ratio.

The basic idea should now be clear: One chooses charges of all Standard Model fermions such that $O(1)$ proto Yukawa couplings give the observed hierarchy in masses due to appropriate powers of the flavon vev. Simultaneously one needs also to ensure that the CKM hierarchies are reproduced.

One choice that gives a reasonably good description of the quark mass hierarchies and the CKM hierarchies is the "master model" from [67]

$$Q(q_1) = +3\,, \qquad Q(q_2) = +2\,, \qquad Q(q_3) = 0\,, \tag{71}$$

$$Q(u_1) = -3\,, \qquad Q(u_2) = -1\,, \qquad Q(u_3) = 0\,, \tag{72}$$

$$Q(d_1) = -3\,, \qquad Q(d_2) = -2\,, \qquad Q(d_3) = -2\,. \tag{73}$$

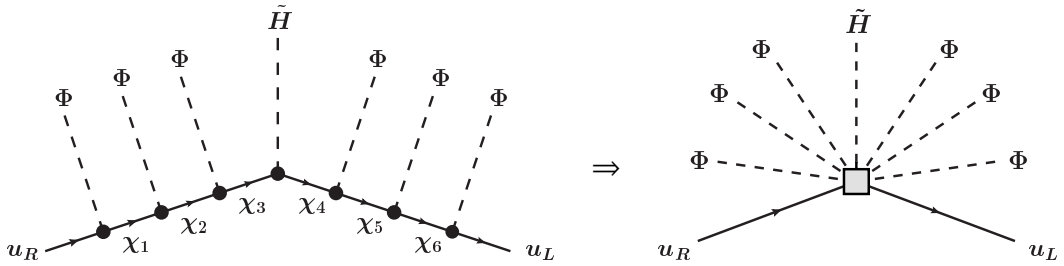

Figure 11: Left: Chain of vectorlike fermions that connect the up quark to the Higgs boson. Right: the corresponding higher dimensional operator from equation (70).

It is a very good exercise to verify that the charge assignments of the master model reproduce the correct scaling of the CKM matrix elements with the Wolfenstein parameter λ if one sets $\langle\Phi\rangle/\Lambda \simeq \lambda$.

Note that the new physics scale Λ is constrained by meson mixing observables to be very high. With the charge assignment of the master model above, one can write, for example, the following unsuppressed operator that contributes to kaon mixing

$$\mathcal{H}_{\text{eff}} \supset \frac{1}{\Lambda^2}(\bar{d}\gamma_\mu P_L s)(\bar{d}\gamma^\mu P_R s) \,. \tag{74}$$

From the discussion in section 2.5 we typically expect that $\Lambda \gtrsim 10^5$ TeV.

The basic setup of spontaneously broken flavor symmetries described above can be extended in various ways. The charged leptons can be incorporated in a straightforward way. It is also possible to introduce more than one $U(1)$ flavor symmetry and work with multiple expansion parameters. Alternatively, one can also use non-abelian flavor symmetries.

5. Decays of B mesons and the "B Anomalies"

Decays of B mesons play a two-fold role in the context of flavor physics and particle physics in general. On the one hand, as mentioned in section 3.2, they are used to determine CKM matrix elements and angles of the unitarity triangle. On the other hand, B decays are also sensitive probes of new physics.

The dominant decay modes of (ground state) B mesons proceed through the weak decay of the b quark into a c quark. Performing a back-of-the-envelope estimate of the decay rate one has in analogy to muon decay

$$\Gamma(b \to c\ell\nu) \simeq \frac{G_F^2}{192\pi^3} m_b^5 |V_{cb}|^2 \,. \tag{75}$$

This corresponds to a sizable lifetime of $\tau_B \sim 10^{-12}$ s and thus implies a potentially high sensitivity to new physics.

5.1 Classification of B Decays

A basic distinction of B decays is between charged current decays and neutral current decays. Charged current decays arise already at the tree level and are the dominant decay modes of B mesons. Neutral currents are loop induced, and the corresponding rates are much smaller. The neutral currents are therefore also referred to as "rare decays".

Estimating the relative size of the amplitudes of various charged and neutral current decays, one finds a clear hierarchy

charged current decays	rare decays	
$A(b \to c) \sim V_{cb} \simeq 4 \times 10^{-2}\,,$	$A(b \to s) \sim \dfrac{1}{16\pi^2} V_{ts}^* V_{tb} \simeq 2 \times 10^{-4}\,,$	(76)
$A(b \to u) \sim V_{ub} \simeq 4 \times 10^{-3}\,,$	$A(b \to d) \sim \dfrac{1}{16\pi^2} V_{td}^* V_{tb} \simeq 5 \times 10^{-5}\,.$	(77)

The main application of the tree-level decay is the precision determination of CKM matrix elements V_{cb} and V_{ub}. Once the CKM elements are known, they can be used to predict the rates for rare decays in the Standard Model. As rare decays are strongly suppressed in the Standard Model, they are potentially sensitive to new physics at very high scales of 10 to 100 TeV.

In parallel to this basic distinction of charged current and neutral current decays, one can further classify B meson decays according to the type of particles in the final state. One distinguishes:

Leptonic Decays: These are decays without any hadron in the final state. In the case of charged B mesons, leptonic decays are tree-level charged current decays. In the case of neutral B mesons, they are rare neutral current decays. Examples include

$$B^+ \to \ell^+ \nu\,, \quad B_s \to \mu^+ \mu^-\,, \quad B^0 \to \mu^+ \mu^-\,, \quad \ldots$$

Radiative Decays: These decays contain a photon in the final state. Both charged and neutral B mesons can decay in that way. In both cases, radiative decays are rare neutral current decays. Examples include

$$B^0 \to K^{*\,0} \gamma\,, \quad B^+ \to K^{*\,+} \gamma\,, \quad B_s \to \phi\gamma\,, \quad \ldots$$

Semileptonic Decays: Semileptonic decays contain leptons and hadrons in the final state. They are available to both charged and neutral B mesons and can proceed either through charged currents or neutral currents. Examples include

$$\text{charged currents:}\;\; B \to D^{(*)} \ell \nu\,, \quad B_s \to K \ell \nu\,, \quad B \to \pi \ell \nu\,, \quad \ldots$$

$$\text{neutral currents:}\;\; B \to K^{(*)} \ell\ell\,, \quad B \to K^{(*)} \nu\nu\,, \quad B_s \to \phi \ell\ell\,, \quad B \to \pi \ell\ell\,, \quad \ldots$$

Hadronic Decays: These are decays with a purely hadronic final state. Because of the large mass of B mesons, there exist hundreds of possibilities for such final states. We will not cover them in these lecture notes, but only remark that the more hadrons are in the final state, the more complicated the theoretical description of the decay becomes.

The various types of decays mentioned above and the corresponding experimentally accessible observables show complementary new physics sensitivity. An effective B physics program thus involves the study of a large number of processes. In the following, we will discuss only a couple of examples. Comprehensive reviews about rare decays as probes of new physics can be found, for example, in [68, 69]

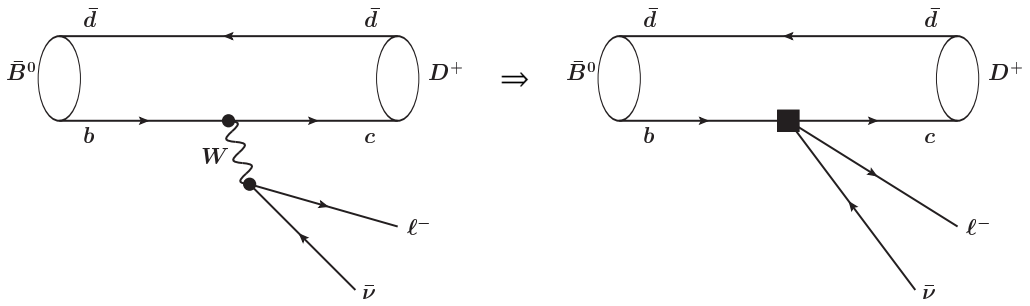

Figure 12: Feynman diagram of the decay $\bar{B}^0 \to D^+\ell^-\bar{\nu}$. Left: Standard Model W boson exchange. Right: Effective Hamiltonian picture.

5.2 Charged Current Example: $B \to D\ell\nu$

The Feynman diagram corresponding to the $B \to D\ell\nu$ decay is shown in the left-hand side of figure 12. The characteristic energy scale of the decay is of the order of the B meson mass or the b quark mass, $m_b \sim 4$ GeV, while the characteristic scale of the weak interactions that mediate the underlying $b \to c\ell\nu$ transition is much larger $m_W \sim 80$ GeV $\gg m_b$. It is thus convenient to integrate out the W boson (and the other weak scale particles, the top, the Z, and the Higgs) and to work in an effective theory framework. This framework is sometimes referred to as the Low Energy Effective Theory (LEFT). In this framework, the W exchange is described by an effective four-fermion contact interaction, shown in the right-hand side of figure 12

$$\mathcal{H}_{\text{eff}} \supset \frac{4G_F}{\sqrt{2}} V_{cb} C (\bar{c}\gamma^\mu P_L b)(\bar{\ell}\gamma_\mu P_L \nu) \; + \; \text{h.c.} \,. \tag{78}$$

In this expression, C is a Wilson coefficient. The normalization factors (the Fermi constant G_F and the CKM matrix element V_{cb}) have been chosen such that integrating out the W boson, one finds $C = 1$ at the tree level in the Standard Model. Based on this effective Hamiltonian, we can calculate the decay amplitude of $\bar{B}^0 \to D^+\ell^-\bar{\nu}$. Neglecting higher-order QED corrections, it factorizes into a leptonic and a hadronic part

$$\langle D^+\ell^-\bar{\nu}|\mathcal{H}_{\text{eff}}|\bar{B}^0\rangle = \frac{4G_F}{\sqrt{2}} V_{cb} C \langle \ell^-\bar{\nu}|\bar{\ell}\gamma_\mu P_L \nu|0\rangle \langle D^+|\bar{c}\gamma^\mu P_L b|\bar{B}^0\rangle \,. \tag{79}$$

The leptonic part is straightforward to evaluate using perturbation theory. On the other hand, the hadronic matrix element $\langle D^+|\bar{c}\gamma^\mu P_L b|\bar{B}^0\rangle$ requires non-perturbative methods. The first step is to parameterize the hadronic matrix element in terms of form factors. Based on the quantum numbers of the B and D mesons (both are pseudoscalars) and the quark current, we find

$$\langle D^+|\bar{c}\gamma^\mu\gamma_5 b|\bar{B}^0\rangle = 0 \,, \quad \langle D^+|\bar{c}\gamma^\mu b|\bar{B}^0\rangle \neq 0 \,. \tag{80}$$

Because of Lorentz invariance, the non-zero matrix element can be written as a linear combination of the B and D meson momenta, p_B^μ and p_D^μ. One possible way to write the matrix element is therefore

$$\langle D^+|\bar{c}\gamma^\mu b|\bar{B}^0\rangle = f_+(q^2)(p_B^\mu + p_D^\mu) + \big(f_0(q^2) - f_+(q^2)\big)\frac{m_B^2 - m_D^2}{q^2} q^\mu \,, \quad \text{with } q^\mu = p_B^\mu - p_D^\mu \,, \tag{81}$$

where the two form factors f_+ and f_0 are functions of the momentum transfer squared q^2. The form factors can be determined using lattice QCD methods. The latest lattice results are summarized in [34].

With the matrix element parameterized as in equation (81), one finds the following expression for the differential decay rate (neglecting terms proportional to lepton masses)

$$\frac{d\Gamma(\bar{B}^0 \to D^+\ell^-\nu)}{dw} = \frac{G_F^2|V_{cb}|^2}{48\pi^3} m_B^2 m_D^3 \left(1+\frac{m_D}{m_B}\right)^2 \eta_{\rm EW}^2 (w^2-1)^{\frac{3}{2}} \mathcal{G}(w)^2 \,, \tag{82}$$

where w is the "recoil parameter" defined as the product of the B and D meson 4 velocities. It can be expressed in terms of the momentum transfer squared in the following way $w = (m_B^2 + m_D^2 - q^2)/(2m_B m_D)$. The factor $\eta_{\rm EW}$ incorporates electro-weak corrections [70] and is very close to 1. The function $\mathcal{G}(w)$ is related to the form factor $f_+(q^2)$ via

$$\mathcal{G}(w)^2 = \frac{4m_D}{m_B}\left(1+\frac{m_D}{m_B}\right)^{-2} f_+^2(q^2) \,. \tag{83}$$

Note that the decay rate in equation (82) receives, in principle, also a contribution from the form factor $f_0(q^2)$. However, this contribution is proportional to the lepton mass squared and can be safely neglected in the case of electrons and muons.

As an application, one uses experimental measurements of the $\bar{B}^0 \to D^+\ell^-\nu$ decay rate and lattice determinations of the form factors to extract the CKM matrix element $|V_{cb}|$. This and other B meson decays feed into the value quoted for $|V_{cb}|$ in equation (57).

5.3 Neutral Current Example: $B_s \to \mu^+\mu^-$

As an example of a flavor changing neutral current decay, we revisit once more the decay $B_s \to \mu^+\mu^-$. Example Feynman diagrams were already shown in figure 1. Also in this example, it is convenient to work in an EFT setup, integrating out the heavy Standard Model particles. In the Standard Model, one finds a single non-negligible operator that describes the effect of the weak interactions

$$\mathcal{H}_{\rm eff} \supset -\frac{4G_F}{\sqrt{2}} V_{tb}V_{ts}^* \frac{e^2}{16\pi^2} C_{10} (\bar{s}\gamma^\alpha P_L b)(\bar{\mu}\gamma_\alpha\gamma_5\mu) \;+\; \text{h.c.} \,. \tag{84}$$

Other operators have either tiny Wilson coefficients (c.f. the discussion in section 2.4) or do not contribute to the $B_s \to \mu^+\mu^-$ decay rate. The normalization factor contains the Fermi constant, the CKM matrix elements relevant for the $b \to s$ transition as well as a loop factor. In that way, the Wilson coefficient C_{10} is an order 1 number. More precisely, one finds in the Standard Model at the 1-loop level

$$C_{10} = \frac{1}{\sin^2\theta_W} Y_0\left(\frac{m_t^2}{m_W^2}\right) \,, \quad \text{with } Y_0(x) = \frac{x}{8}\left(\frac{4-x}{1-x} + \frac{3x\log x}{(1-x)^2}\right) \,, \tag{85}$$

where θ_W is the weak mixing angle, and Y_0 is a 1-loop function [71, 72]. Numerically, $C_{10} \simeq -4$. The subscript "10" on the Wilson coefficient suggests that there are many additional operators related to neutral current $b \to s$ decays. Indeed several additional operators are relevant for decays like $B \to K^*\gamma$ or $B \to K^{(*)}\mu^+\mu^-$. A comprehensive review of the effective Hamiltonian for flavor-changing neutral current decays is given in [25, 72].

Next, we calculate the $B_s \to \mu^+\mu^-$ decay amplitude

$$\langle \mu^+\mu^-|\mathcal{H}_{\text{eff}}|\bar{B}_s\rangle = \frac{4G_F}{\sqrt{2}} V_{tb}V_{ts}^* \frac{e^2}{16\pi^2} C_{10}\langle \mu^+\mu^-|\mu\gamma_\alpha\gamma_5\mu|0\rangle\langle 0|\bar{s}\gamma^\alpha P_L b|\bar{B}_s\rangle \,. \tag{86}$$

The leptonic part is again straightforward. The hadronic matrix element is simpler than in the example of the previous section 5.2, as it involves only a single meson that transitions to the vacuum. Based on the quantum numbers of the B_s meson, the vacuum, and the involved current, we find

$$\langle 0|\bar{s}\gamma^\alpha b|\bar{B}_s\rangle = 0\,, \quad \langle 0|\bar{s}\gamma^\alpha\gamma_5 b|\bar{B}_s\rangle \neq 0\,. \tag{87}$$

Using Lorentz invariance, the non-zero matrix element has to be proportional to the B_s meson momentum p_{B_s}

$$\langle 0|\bar{s}\gamma^\alpha\gamma_5 b|\bar{B}_s\rangle = i f_{B_s} p_{B_s}^\alpha \,. \tag{88}$$

The proportionality factor f_{B_s} is known as the B_s meson decay constant. Despite it being a non-perturbative object, the B_s meson decay constant is known with sub-percent precision from lattice QCD calculations $f_{B_s} = 230.3(1.3)$ MeV [34].

We then arrive at the following expression for the $B_s \to \mu^+\mu^-$ branching ratio

$$\text{BR}(B_s \to \mu^+\mu^-)_{\text{SM}} = \tau_{B_s} \frac{G_F^2}{\pi} m_{B_s} f_{B_s}^2 m_\mu^2 \frac{\alpha^2}{16\pi^2} |V_{tb}V_{ts}^*|^2 \frac{Y_0^2(x_t)}{\sin^4\theta_W} \,. \tag{89}$$

An important aspect is the proportionality of the branching ratio to the muon mass squared m_μ^2. This helicity suppression is reminiscent of leptonic pion decay, $\pi \to \mu\nu$, which features an analogous suppression.

State-of-the-art Standard Model predictions of the $B_s \to \mu^+\mu^-$ branching ratio take into account next-to-leading order electroweak corrections and next-to-next-to-leading order QCD corrections [73], QED corrections [74], as well as the small lifetime difference of the B_s meson mass eigenstates [75]. The Standard Model prediction $\text{BR}(B_s \to \mu^+\mu^-)_{\text{SM}} = (3.66 \pm 0.23) \times 10^{-9}$ [74] has an uncertainty below 10%. The uncertainty is dominated by the uncertainty on the CKM matrix input. Comparing the Standard Model prediction with the experimental measurements of the branching ratio, one can test if there are any new physics contributions mediating the $B_s \to \mu^+\mu^-$ decay.

With a branching ratio of $O(10^{-9})$, the $B_s \to \mu^+\mu^-$ decay is truly a rare decay. From the experimental side, one searches for a $\mu^+\mu^-$ resonance with the mass of the B_s meson, $m_{B_s} \simeq 5.37$ GeV. The first observation was achieved in 2014, combining results from LHCb and CMS [76]. The current world average combines results from LHCb, CMS, and ATLAS and reads $\text{BR}(B_s \to \mu^+\mu^-)_{\text{exp}} = (3.45 \pm 0.29) \times 10^{-9}$ [33] and is in excellent agreement with the Standard Model prediction. The di-muon invariant mass spectrum of the most recent CMS analysis [13] is shown in figure 13. The prominent $B_s \to \mu^+\mu^-$ peak is clearly visible.

5.4 Semileptonic Rare B Decays and Lepton Flavor Universality Tests

Compared to the leptonic decay $B_s \to \mu^+\mu^-$ discussed in the previous section 5.3, semileptonic rare decays like $B \to K\ell\ell$, $B \to K^*\ell\ell$, and $B_s \to \phi\ell\ell$ are considerably more complicated to describe theoretically. In particular, one needs to control additional hadronic effects that are not captured

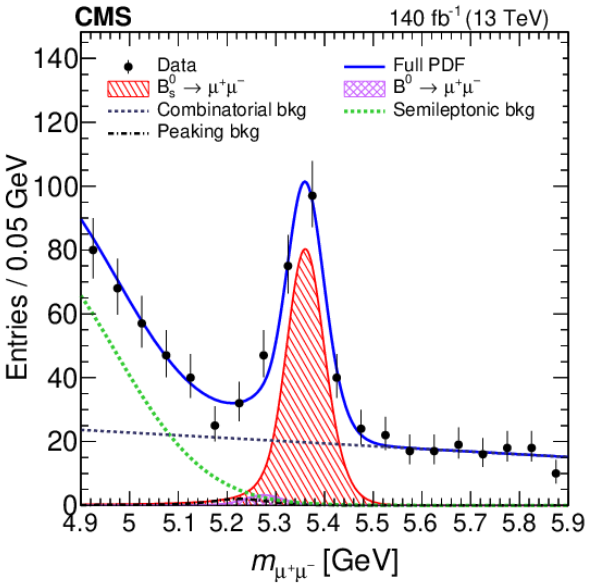

Figure 13: The di-muon invariant mass distribution in the vicinity of the B_s mass as observed by CMS [13].

by local form factors. These additional hadronic effects are sometimes referred to as "non-local contributions" or also "charm loop contributions", and we will not discuss them here in detail. Schematically, an amplitude for the decay $B \to K^* \mu^+ \mu^-$ can be written as

$$A(B \to K^* \mu^+ \mu^-)^{L,R}_{\lambda} \propto (C_9 \pm C_{10}) \mathcal{F}_\lambda(q^2) + \frac{2 m_b m_B}{q^2} \left(C_7 \mathcal{F}^T_\lambda(q^2) - 16\pi^2 \frac{m_B}{m_b} \mathcal{H}_\lambda(q^2) \right) . \tag{90}$$

The subscript λ denotes the polarization of the K^*, C_7, C_9, C_{10} are the Wilson coefficients of dimension-6 operators and $\mathcal{F}_\lambda$, $\mathcal{F}^T_\lambda$ are combinations of local form factors, similar to f_0 and f_+ introduced in section 5.2. The non-local contributions are parameterized by $\mathcal{H}_\lambda(q^2)$. They contain, for example, the process with an intermediate narrow charmonium resonance $B \to K^* J\psi \to K^* \mu^+ \mu^-$ as sketched in figure 14 taken from [77]. For q^2 sufficiently below the charmonium resonances, one might expect that the non-local contributions give only a small correction. Nevertheless, also in the low q^2 region, both the non-local contributions and the local form factors give sizable theoretical uncertainties. Detailed discussions can be found, for example, in [78, 79].

A clever way to remove dependence on the form factors and the non-local contributions is to consider so-called lepton flavor universality (LFU) ratios [80], for example,

$$R_K = \frac{\mathrm{BR}(B \to K \mu^+ \mu^-)}{\mathrm{BR}(B \to K e^+ e^-)} , \qquad R_{K^*} = \frac{\mathrm{BR}(B \to K^* \mu^+ \mu^-)}{\mathrm{BR}(B \to K^* e^+ e^-)} . \tag{91}$$

Because the muon and the electron mass are both small compared to the B meson mass, they can be neglected to a good approximation. As the electroweak interactions are lepton flavor universal, the Standard Model predicts $R_K \simeq R_{K^*} \simeq 1$ with percent level precision [81].

The observables R_K and R_{K^*} are clean "null tests" of the Standard Model. A significant deviation from 1 would be a clear sign of new physics (or an unknown experimental systematic).

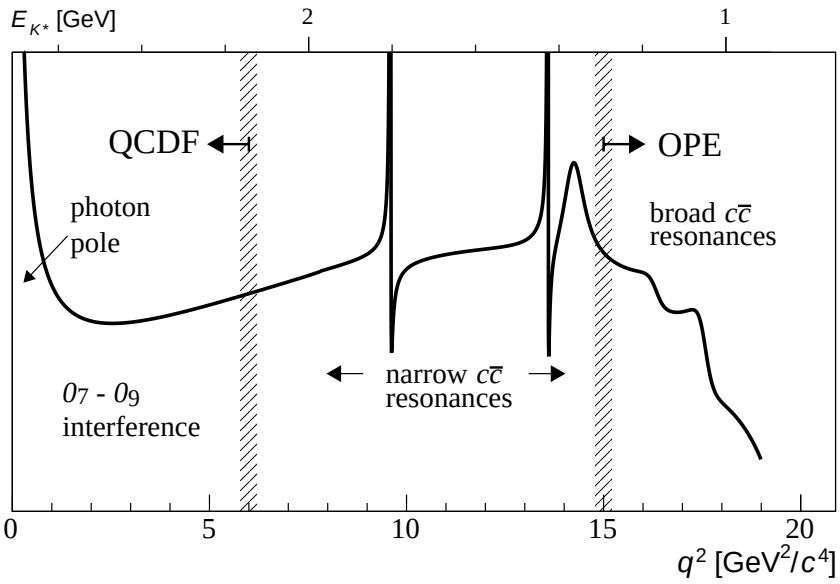

Figure 14: A sketch of the di-muon invariant mass squared (q^2) distribution of the differential decay rate of $B \to K^* \mu^+ \mu^-$. (Plot taken from [77].)

Intriguingly, for a long time, LHCb measurements of LFU ratios gave results significantly below the Standard Model prediction [82, 83], creating considerable excitement in the particle physics community. The large flavor model building undertaking that was motivated by the hints for lepton flavor universality violation is summarized, for example, in [53]. The most recent update by LHCb from December 2022, however, gives results that are fully compatible with the Standard Model predictions $\simeq 1$ [84, 85]

$$\text{low-}q^2 \begin{cases} R_K = 0.994\ ^{+0.090}_{-0.082}(\text{stat})\ ^{+0.029}_{-0.027}(\text{sys})\,, \\ R_{K^*} = 0.927\ ^{+0.093}_{-0.087}(\text{stat})\ ^{+0.036}_{-0.035}(\text{sys})\,, \end{cases}$$

$$\text{central-}q^2 \begin{cases} R_K = 0.949\ ^{+0.042}_{-0.041}(\text{stat})\ ^{+0.022}_{-0.022}(\text{sys})\,, \\ R_{K^*} = 1.027\ ^{+0.072}_{-0.068}(\text{stat})\ ^{+0.027}_{-0.026}(\text{sys})\,, \end{cases}$$

where (stat) and (sys) correspond to statistical and systematic uncertainties, respectively. "low-q^2" and "high-q^2" refers to the q^2 bins $[0.1, 1.1]$ GeV^2 and $[1.1, 6]$ GeV^2, respectively.

These most recent R_K and R_{K^*} results from LHCb are also illustrated in figure 15. These results can be used to constrain new physics that couples non-universally to muons and electrons. After the high-luminosity run of the LHC, one can expect measurements of R_K and R_{K^*} with percent-level precision [10]. Also Belle II might reach comparable precision [11].

Lepton flavor universality is also probed in semi-leptonic charged current B decays. Of particular interest are the observables R_D and R_{D^*} defined as

$$R_D = \frac{\text{BR}(B \to D\tau\nu)}{\text{BR}(B \to D\ell\nu)}\,, \qquad R_{D^*} = \frac{\text{BR}(B \to D^*\tau\nu)}{\text{BR}(B \to D^*\ell\nu)}\,, \tag{92}$$

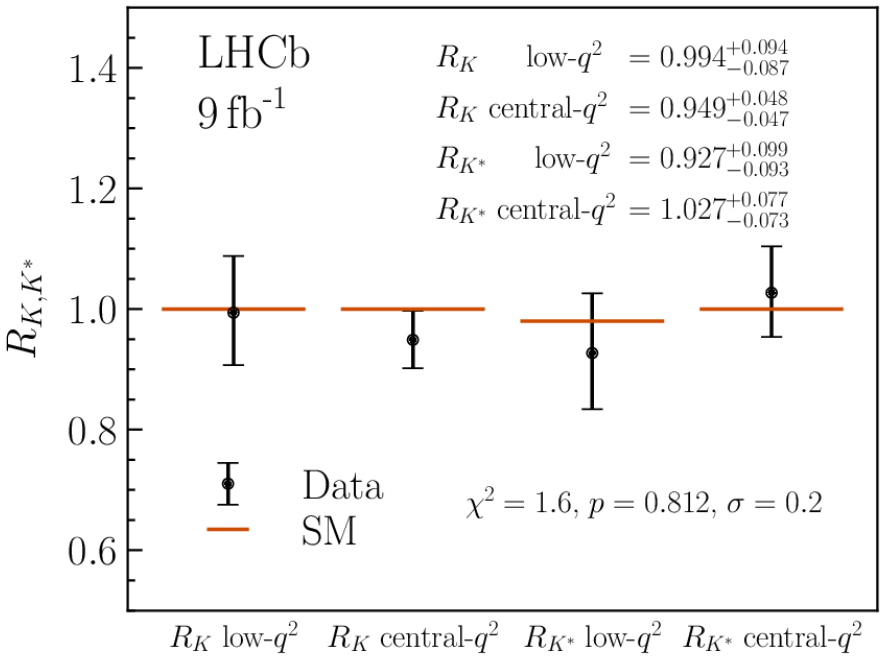

Figure 15: LHCb measurements of the lepton flavor universality ratios R_K and R_{K^*} in two different bins of di-lepton invariant mass squared. (Plot taken from [85].)

where ℓ refers to the light leptons. LHCb results on R_D and R_{D^*}, are based on final states with a muon, $\ell = \mu$, while results from the B factories average over muons and electrons, $\ell = e, \mu$. The decay rates into muons and electrons, $B \to D^* e\nu$ and $B \to D^* \mu\nu$, are experimentally known to be universal at the percent level [86].

The Standard Model predictions for R_D and R_{D^*} are not close to 1. Due to the large mass of the tau, $m_\tau \gg m_\mu, m_e$, the phase space effects are non-negligible and give a decay rate into taus that is a factor of 3-4 below the decay rate into the light leptons. In contrast to R_K and R_{K^*}, hadronic uncertainties do not fully cancel but are still found to be under good control. The heavy flavor averaging group provides the following Standard Model predictions that have percent level accuracy [33]

$$R_D^{\rm SM} = 0.298 \pm 0.004\,, \qquad R_{D^*}^{\rm SM} = 0.254 \pm 0.005\,. \tag{93}$$

The uncertainty is mainly driven by ratios of form factors that have to be calculated on the lattice or determined using data-driven methods [87].

On the experimental side, several results hint at an enhanced rate for the final state with taus. In particular, the 2012 result from BaBar [88] finds values for both R_D and R_{D^*} that are significantly larger than the Standard Model prediction. Combining the BaBar result with more recent analyses from Belle and LHCb, one finds the following world average [33]

$$R_D^{\rm exp} = 0.356 \pm 0.029\,, \qquad R_{D^*}^{\rm exp} = 0.284 \pm 0.013\,, \tag{94}$$

with an error correlation of -37%. This result corresponds to a combined 3.2σ tension with the Standard Model prediction. More decays with taus are observed than expected. The situation is

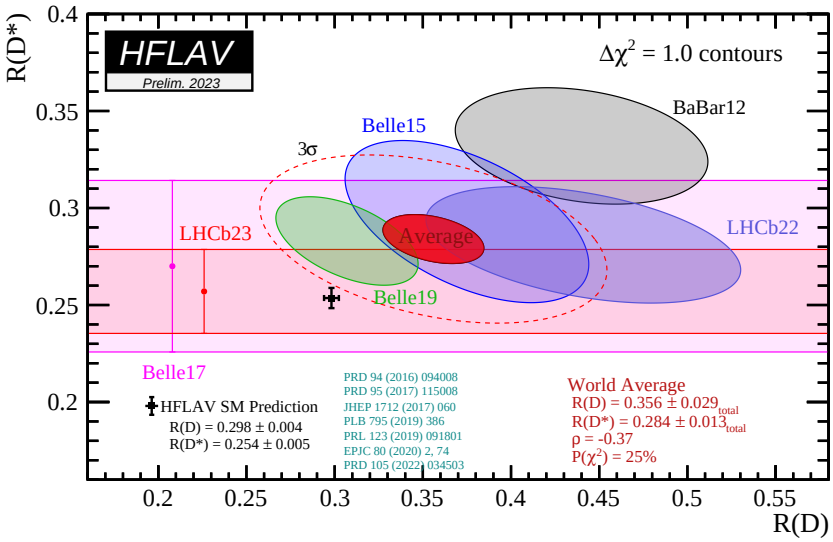

Figure 16: Summary of R_D and R_{D^*} measurements by the heavy flavor averaging group [33].

summarized in figure 16. LHCb and Belle II are expected to improve the measurements considerably and to measure R_D and R_{D^*} with percent-level precision [10, 11].

5.5 The Rare B Anomalies and Their Interpretation

While the latest experimental results on the lepton flavor universality ratios R_K and R_{K^*} are in good agreement with Standard Model predictions, there are a number of rare B decay properties for which measurements and Standard Model predictions do not agree very well:

- First, the absolute branching ratios of the decays $B \to K\mu^+\mu^-$, $B \to K^*\mu^+\mu^-$, and $B_s \to \phi\mu^+\mu^-$ are consistently below their Standard Model predictions over a broad range of q^2. Given that R_K, $R_{K^*} \simeq 1$, this means that also the decays with electrons in the final state are below the values predicted in the Standard Model.

- Second, the measured angular distribution of the decay products in the $B \to K^*\mu^+\mu^-$ decay does not agree well with the Standard Model prediction. This is often referred to as the "P_5' anomaly". The P_5' observable was introduced in [89] and can be understood as a combination of angular moments of the $B \to K^*\mu^+\mu^-$ decay distribution. Most other angular observables agree reasonably well with Standard Model predictions.

Collectively, these discrepancies are referred to as "rare B decay anomalies". It is important to note that both the absolute branching ratios and the $B \to K^*\mu^+\mu^-$ angular distribution are subject to hadronic uncertainties that are difficult to estimate reliably. Statements about the significance of the discrepancies are based on models of the hadronic contributions and have to be interpreted cautiously. Lots of effort is being dedicated to understanding the hadronic contributions better and to devising methods to determine them from data, see for example [79, 90–93].

Assuming that existing models capture the hadronic physics in a reliable way, one can interpret the discrepancies as signs of new physics. The standard procedure for identifying which type of

new physics could be responsible starts with a "model independent new physics analysis". The minimal assumption that one makes is that the new physics is heavy compared to the B mesons. In that case, one can formulate the new physics effects model independently using an effective field theory. The usual approach is to consider new physics contributions to all dimension-6 operators that contribute to $b \to s\ell\ell$ decays at the tree level. The corresponding effective Hamiltonian reads

$$\mathcal{H}_{\text{eff}} = -\frac{4G_F}{\sqrt{2}} V_{tb} V_{ts}^* \frac{e^2}{16\pi^2} \sum_i C_i O_i \ + \text{h.c.}\,, \tag{95}$$

We used the same normalization as in the effective Hamiltonian for the $B_s \to \mu^+\mu^-$ decay in equation (86). However, in contrast to equation (86) we now include all operators that contribute to leptonic, semileptonic, and radiative $b \to s$ decays. Explicitly, the operators are

$$O_7 = \frac{m_b}{e}(\bar{s}\sigma_{\mu\nu}P_R b)F^{\mu\nu}\,, \qquad O_7' = \frac{m_b}{e}(\bar{s}\sigma_{\mu\nu}P_L b)F^{\mu\nu}\,, \tag{96}$$

$$O_9 = (\bar{s}\gamma_\mu P_L b)(\bar{\ell}\gamma^\mu \ell)\,, \qquad O_9' = (\bar{s}\gamma_\mu P_R b)(\bar{\ell}\gamma^\mu \ell)\,, \tag{97}$$

$$O_{10} = (\bar{s}\gamma_\mu P_L b)(\bar{\ell}\gamma^\mu\gamma_5 \ell)\,, \qquad O_{10}' = (\bar{s}\gamma_\mu P_R b)(\bar{\ell}\gamma^\mu\gamma_5 \ell)\,, \tag{98}$$

$$O_S = (\bar{s}P_R b)(\bar{\ell}\ell)\,, \qquad O_S' = (\bar{s}P_L b)(\bar{\ell}\ell)\,, \tag{99}$$

$$O_P = (\bar{s}P_R b)(\bar{\ell}\gamma_5 \ell)\,, \qquad O_P' = (\bar{s}P_L b)(\bar{\ell}\gamma_5 \ell)\,, \tag{100}$$

$$O_T = (\bar{s}\sigma_{\mu\nu}P_R b)(\bar{\ell}\sigma^{\mu\nu} \ell)\,, \qquad O_T' = (\bar{s}\sigma_{\mu\nu}P_L b)(\bar{\ell}\sigma^{\mu\nu} \ell)\,. \tag{101}$$

The set of operators consists of dipole operators O_7, O_7' and four-fermion contact interactions. Note that not all of the above operators are compatible with the $SU(2)_L \times U(1)_Y$ gauge symmetry of the Standard Model. Some of the operators are thus secretly dimension-8 and expected to be suppressed. It is a good exercise to identify these operators.

The Wilson coefficients of the operators can be decomposed into a Standard Model part C_i^{SM} and a new physics part ΔC_i

$$C_i = C_i^{\text{SM}} + \Delta C_i\,. \tag{102}$$

The non-negligible Wilson coefficients in the Standard Model are $C_7^{\text{SM}} \simeq -0.3$, $C_9^{\text{SM}} \simeq 4$, and (as already mentioned in section 5.3) $C_{10}^{\text{SM}} \simeq -4$.

The next step is then to express all relevant observables, like the rare B decay branching ratios, angular observables, and lepton flavor universality ratios as functions of the new physics Wilson coefficients ΔC_i. Finally, one fits the coefficients ΔC_i to data and sees if any non-zero values are preferred. A software package that has been designed to perform precisely these steps is `flavio` [94].

Examples of global Wilson coefficient fits that take into account the most recent experimental results are shown in the plots of figure 17 that were created with `flavio`.

The plot on the left-hand side shows a fit to muon-specific new physics contributions to C_9 and C_{10}. The Standard Model point corresponds to $\Delta C_9^\mu = \Delta C_{10}^\mu = 0$. The yellow horizontal band shows the constraint from $B_s \to \mu^+\mu^-$ (see section 5.3) and the blue band to the combination of the lepton flavor universality ratios R_K and R_{K^*}. Only these theoretically clean observables are considered, while the other $b \to s\mu\mu$ observables that are sensitive to hadronic effects are ignored. The combination is shown in red. The red region is compatible with the Standard Model and limits the amount of new physics that is allowed. The black dashed line shows the expectation after

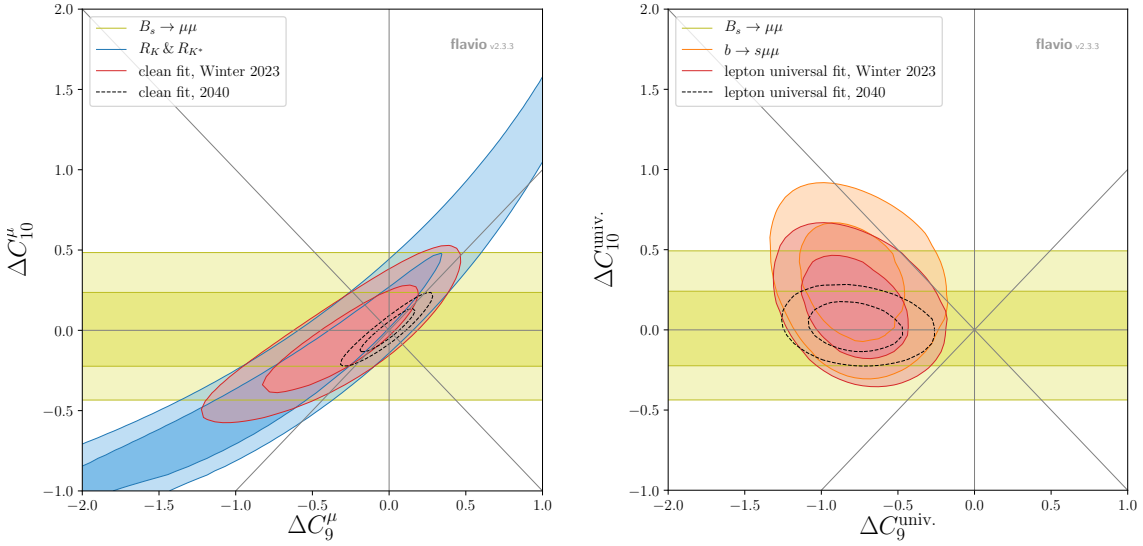

Figure 17: Left: Rare B decay fit in the plane of muon-specific new physics contributions to C_9 and C_{10}, including only theoretically clean observables. Right: Rare B decay fit in the plane of lepton universal new physics contributions to the Wilson coefficients C_9 and C_{10}. (Plots taken from [95]. See [93, 96–100] for other similar recent studies.)

the high-luminosity run of the LHC, assuming that R_K, R_{K^*}, and $B_s \to \mu^+\mu^-$ will continue to agree with Standard Model predictions. One can observe a significant improvement in the expected constraint.

The plot on the right-hand side shows a similar fit, but this time for lepton flavor universal new physics contributions to the Wilson coefficients C_9 and C_{10}. The orange ellipse corresponds to the combination of all available data on the rare semileptonic $b \to s\mu\mu$ decays, including $B \to K\mu^+\mu^-$, $B \to K^*\mu^+\mu^-$, $B_s \to \phi\mu^+\mu^-$, and the baryon decay $\Lambda_b \to \Lambda\mu^+\mu^-$. The ratios R_K and R_{K^*} do not give any constraints by construction, as the new physics is assumed to be lepton flavor universal. The global combination in red shows a preference for lepton universal new physics by approximately 3σ. As mentioned previously, the significance depends strongly on the modeling of the hadronic contributions to the $b \to s\ell\ell$ decays. While the precise significance is debatable, a negative lepton universal shift of the Wilson coefficient C_9 improves the fit to the data and addresses the rare B anomalies.

One finds that adding other Wilson coefficients beyond $\Delta C_9^{\text{univ.}}$ does not significantly improve the fit further. Also, other Wilson coefficients by themselves do not give a good fit to the data.

Having identified a possible new physics origin of the rare B decay anomalies in the form of a four-fermion contact interaction, the next question is which is the new physics scale associated with the anomalies? In this context, it is convenient to reparameterize the Wilson coefficients in the effective Hamiltonian (95) in the following way

$$\frac{4G_F}{\sqrt{2}} V_{tb} V_{ts}^* \frac{e^2}{16\pi^2} |\Delta C_9| = \frac{1}{\Lambda_{\text{NP}}^2} \,. \tag{103}$$

This gives a new physics scale of $\Lambda_{\text{NP}} \simeq 35$ TeV. This scale can be interpreted as the characteristic mass scale of new physics particles that contribute to $b \to s\ell\ell$ decays at the tree level and that have

$O(1)$ flavor violating couplings. This new physics scale is at an interesting level. On the one hand, $\Lambda_{\rm NP}$ is far above the electroweak scale, and it is conceivable that whatever new physics might be behind the rare B decay anomalies, it is outside the direct reach of the LHC. On the other hand, the scale is sufficiently low that the new physics might be within reach of future colliders. A plethora of new physics models have been proposed that give the effective operator preferred by the global fits. This includes models with Z' gauge bosons and models with leptoquarks. For a recent review see [53].

If there is indeed new physics behind the rare B decay anomalies, one can expect that Belle II will find supporting evidence from measurements of the inclusive decay $B \to X_s \ell^+ \ell^-$, which is theoretically under better control than the exclusive decays measured by LHCb [101, 102]. Moreover, one generically expects correlated effects in related processes like $b \to d\ell\ell$ decays [103, 104] (which can be measured precisely by LHCb during the high luminosity phase), $b \to s\nu\bar{\nu}$ decays [105, 106] (which will be measured precisely at Belle II), and $b \to s\tau\tau$ decays [107, 108] (which could be accessed at future circular e^+e^- colliders running on the Z pole). On the energy frontier, both a high-energy muon collider and a 100 TeV hadron collider have excellent prospects to probe the new physics that could be behind the rare B decay anomalies [95, 109–113].

Acknowledgements

I would like to thank Jiji Fan, Stefania Gori, and Liantao Wang for the invitation to teach at TASI 2022. The work of W.A. is supported by DOE grant DE-SC0010107. This write-up was partially completed at the Aspen Center for Physics, which is supported by National Science Foundation grant PHY-2210452.

References

[1] S. L. Glashow, J. Iliopoulos and L. Maiani, "Weak Interactions with Lepton-Hadron Symmetry," Phys. Rev. D **2**, 1285-1292 (1970) doi:10.1103/PhysRevD.2.1285

[2] M. K. Gaillard, B. W. Lee and J. L. Rosner, "Search for Charm," Rev. Mod. Phys. **47**, 277-310 (1975) doi:10.1103/RevModPhys.47.277

[3] M. Kobayashi and T. Maskawa, "CP Violation in the Renormalizable Theory of Weak Interaction," Prog. Theor. Phys. **49**, 652-657 (1973) doi:10.1143/PTP.49.652

[4] J. R. Ellis, J. S. Hagelin and S. Rudaz, "Reexamination of the Standard Model in the Light of B Meson Mixing," Phys. Lett. B **192**, 201-206 (1987) doi:10.1016/0370-2693(87)91168-3

[5] I. I. Y. Bigi and A. I. Sanda, "From a New Smell to a New Flavor: $B_d - \bar{B}_d$ Mixing, CP Violation and New Physics," Phys. Lett. B **194**, 307-311 (1987) doi:10.1016/0370-2693(87)90548-X

[6] V. D. Barger, T. Han, D. V. Nanopoulos and R. J. N. Phillips, "$B^0 - \bar{B}^0$ Oscillations and the Top Quark Mass," Phys. Lett. B **194**, 312 (1987) doi:10.1016/0370-2693(87)90549-1

[7] H. Harari and Y. Nir, "$B^0 - \bar{B}^0$ Mixing and Relations Among Quark Masses, Angles and Phases," Phys. Lett. B **195**, 586-592 (1987) doi:10.1016/0370-2693(87)91578-4

[8] G. Altarelli and P. J. Franzini, "$B^0 - \bar{B}^0$ Mixing Within and Beyond the Standard Model," Z. Phys. C **37**, 271 (1988) doi:10.1007/BF01579913

[9] A. A. Alves, Jr. *et al.* [LHCb], "The LHCb Detector at the LHC," JINST **3**, S08005 (2008) doi:10.1088/1748-0221/3/08/S08005

[10] R. Aaij *et al.* [LHCb], "Physics case for an LHCb Upgrade II - Opportunities in flavour physics, and beyond, in the HL-LHC era," [arXiv:1808.08865 [hep-ex]].

[11] E. Kou *et al.* [Belle-II], "The Belle II Physics Book," PTEP **2019**, no.12, 123C01 (2019) [erratum: PTEP **2020**, no.2, 029201 (2020)] doi:10.1093/ptep/ptz106 [arXiv:1808.10567 [hep-ex]].

[12] M. Aaboud *et al.* [ATLAS], "Study of the rare decays of B_s^0 and B^0 mesons into muon pairs using data collected during 2015 and 2016 with the ATLAS detector," JHEP **04**, 098 (2019) doi:10.1007/JHEP04(2019)098 [arXiv:1812.03017 [hep-ex]].

[13] A. Tumasyan *et al.* [CMS], "Measurement of the $B_s^0 \to \mu^+\mu^-$ decay properties and search for the $B^0 \to \mu^+\mu^-$ decay in proton-proton collisions at $\sqrt{s}$ = 13 TeV," Phys. Lett. B **842**, 137955 (2023) doi:10.1016/j.physletb.2023.137955 [arXiv:2212.10311 [hep-ex]].

[14] A. J. Bevan *et al.* [BaBar and Belle], "The Physics of the B Factories," Eur. Phys. J. C **74**, 3026 (2014) doi:10.1140/epjc/s10052-014-3026-9 [arXiv:1406.6311 [hep-ex]].

[15] E. Cortina Gil *et al.* [NA62], "The Beam and detector of the NA62 experiment at CERN," JINST **12**, no.05, P05025 (2017) doi:10.1088/1748-0221/12/05/P05025 [arXiv:1703.08501 [physics.ins-det]].

[16] E. Cortina Gil *et al.* [NA62], "Measurement of the very rare $K^+ \to \pi^+\nu\bar{\nu}$ decay," JHEP **06**, 093 (2021) doi:10.1007/JHEP06(2021)093 [arXiv:2103.15389 [hep-ex]].

[17] T. Yamanaka [KOTO], "The J-PARC KOTO experiment," PTEP **2012**, 02B006 (2012) doi:10.1093/ptep/pts057

[18] J. K. Ahn *et al.* [KOTO], "Study of the $K_L \to \pi^0\nu\bar{\nu}$ Decay at the J-PARC KOTO Experiment," Phys. Rev. Lett. **126**, no.12, 121801 (2021) doi:10.1103/PhysRevLett.126.121801 [arXiv:2012.07571 [hep-ex]].

[19] A. M. Baldini *et al.* [MEG II], "The design of the MEG II experiment," Eur. Phys. J. C **78**, no.5, 380 (2018) doi:10.1140/epjc/s10052-018-5845-6 [arXiv:1801.04688 [physics.ins-det]].

[20] L. Bartoszek *et al.* [Mu2e], "Mu2e Technical Design Report," doi:10.2172/1172555 [arXiv:1501.05241 [physics.ins-det]].

[21] A. Abada *et al.* [FCC], "FCC-ee: The Lepton Collider: Future Circular Collider Conceptual Design Report Volume 2," Eur. Phys. J. ST **228**, no.2, 261-623 (2019) doi:10.1140/epjst/e2019-900045-4

[22] G. Bernardi, E. Brost, D. Denisov, G. Landsberg, M. Aleksa, D. d'Enterria, P. Janot, M. L. Mangano, M. Selvaggi and F. Zimmermann, *et al.* "The Future Circular Collider: a Summary for the US 2021 Snowmass Process," [arXiv:2203.06520 [hep-ex]].

[23] J. B. Guimarães da Costa *et al.* [CEPC Study Group], "CEPC Conceptual Design Report: Volume 2 - Physics & Detector," [arXiv:1811.10545 [hep-ex]].

[24] H. Cheng *et al.* [CEPC Physics Study Group], "The Physics potential of the CEPC. Prepared for the US Snowmass Community Planning Exercise (Snowmass 2021)," [arXiv:2205.08553 [hep-ph]].

[25] A. J. Buras, "Weak Hamiltonian, CP violation and rare decays," [arXiv:hep-ph/9806471 [hep-ph]].

[26] O. Gedalia and G. Perez, "Flavor Physics," doi:10.1142/9789814327183_0006 [arXiv:1005.3106 [hep-ph]].

[27] B. Grinstein, "TASI-2013 Lectures on Flavor Physics," [arXiv:1501.05283 [hep-ph]].

[28] Z. Ligeti, "TASI Lectures on Flavor Physics," doi:10.1142/9789814678766_0006 [arXiv:1502.01372 [hep-ph]].

[29] Y. Grossman and P. Tanedo, "Just a Taste: Lectures on Flavor Physics," doi:10.1142/9789813233348_0004 [arXiv:1711.03624 [hep-ph]].

[30] J. Zupan, "Introduction to flavour physics," CERN Yellow Rep. School Proc. **6**, 181-212 (2019) doi:10.23730/CYRSP-2019-006.181 [arXiv:1903.05062 [hep-ph]].

[31] L. Silvestrini, "Effective Theories for Quark Flavour Physics," doi:10.1093/oso/9780198855743.003.0008 [arXiv:1905.00798 [hep-ph]].

[32] S. Gori, "TASI lectures on flavor physics," PoS **TASI2018**, 013 (2019)

[33] Y. S. Amhis *et al.* [Heavy Flavor Averaging Group and HFLAV], "Averages of b-hadron, c-hadron, and τ-lepton properties as of 2021," Phys. Rev. D **107**, no.5, 052008 (2023) doi:10.1103/PhysRevD.107.052008 [arXiv:2206.07501 [hep-ex]]. Online update at https://hflav.web.cern.ch/

[34] Y. Aoki *et al.* [Flavour Lattice Averaging Group (FLAG)], "FLAG Review 2021," Eur. Phys. J. C **82**, no.10, 869 (2022) doi:10.1140/epjc/s10052-022-10536-1 [arXiv:2111.09849 [hep-lat]]. Online update at http://flag.unibe.ch

[35] S. Pascoli, "Neutrino physics," CERN Yellow Rep. School Proc. **6**, 213-259 (2019) doi:10.23730/CYRSP-2019-006.213

[36] M. C. Gonzalez-Garcia, "Neutrino physics," CERN Yellow Rep. School Proc. **5**, 85 (2022) doi:10.23730/CYRSP-2021-005.85

[37] N. Cabibbo, "Unitary Symmetry and Leptonic Decays," Phys. Rev. Lett. **10**, 531-533 (1963) doi:10.1103/PhysRevLett.10.531

[38] https://www.symmetrymagazine.org/article/june-2013/the-march-of-the-penguin-diagrams

[39] B. Grzadkowski, M. Iskrzynski, M. Misiak and J. Rosiek, "Dimension-Six Terms in the Standard Model Lagrangian," JHEP **10**, 085 (2010) doi:10.1007/JHEP10(2010)085 [arXiv:1008.4884 [hep-ph]].

[40] A. J. Buras, M. Misiak and J. Urban, "Two loop QCD anomalous dimensions of flavor changing four quark operators within and beyond the standard model," Nucl. Phys. B **586**, 397-426 (2000) doi:10.1016/S0550-3213(00)00437-5 [arXiv:hep-ph/0005183 [hep-ph]].

[41] M. Ciuchini, E. Franco, V. Lubicz, G. Martinelli, I. Scimemi and L. Silvestrini, "Next-to-leading order QCD corrections to $\Delta F = 2$ effective Hamiltonians," Nucl. Phys. B **523**, 501-525 (1998) doi:10.1016/S0550-3213(98)00161-8 [arXiv:hep-ph/9711402 [hep-ph]].

[42] M. Bona *et al.* [UTfit], "Model-independent constraints on $\Delta F = 2$ operators and the scale of new physics," JHEP **03**, 049 (2008) doi:10.1088/1126-6708/2008/03/049 [arXiv:0707.0636 [hep-ph]]. Update from talk by Marcella Bona at ICHEP 2022, https://agenda.infn.it/event/28874/contributions/171430/

[43] F. Gabbiani, E. Gabrielli, A. Masiero and L. Silvestrini, "A Complete analysis of FCNC and CP constraints in general SUSY extensions of the standard model," Nucl. Phys. B **477**, 321-352 (1996) doi:10.1016/0550-3213(96)00390-2 [arXiv:hep-ph/9604387 [hep-ph]].

[44] W. Altmannshofer, A. J. Buras, S. Gori, P. Paradisi and D. M. Straub, "Anatomy and Phenomenology of FCNC and CPV Effects in SUSY Theories," Nucl. Phys. B **830**, 17-94 (2010) doi:10.1016/j.nuclphysb.2009.12.019 [arXiv:0909.1333 [hep-ph]].

[45] C. Csaki, A. Falkowski and A. Weiler, "The Flavor of the Composite Pseudo-Goldstone Higgs," JHEP **09**, 008 (2008) doi:10.1088/1126-6708/2008/09/008 [arXiv:0804.1954 [hep-ph]].

[46] M. Blanke, A. J. Buras, B. Duling, S. Gori and A. Weiler, "$\Delta F = 2$ Observables and Fine-Tuning in a Warped Extra Dimension with Custodial Protection," JHEP **03**, 001 (2009) doi:10.1088/1126-6708/2009/03/001 [arXiv:0809.1073 [hep-ph]].

[47] Y. Nir and N. Seiberg, "Should squarks be degenerate?," Phys. Lett. B **309**, 337-343 (1993) doi:10.1016/0370-2693(93)90942-B [arXiv:hep-ph/9304307 [hep-ph]].

[48] G. D'Ambrosio, G. F. Giudice, G. Isidori and A. Strumia, "Minimal flavor violation: An Effective field theory approach," Nucl. Phys. B **645**, 155-187 (2002) doi:10.1016/S0550-3213(02)00836-2 [arXiv:hep-ph/0207036 [hep-ph]].

[49] E. Tiesinga, P. J. Mohr, D. B. Newell and B. N. Taylor, "CODATA recommended values of the fundamental physical constants: 2018*," Rev. Mod. Phys. **93**, no.2, 025010 (2021) doi:10.1103/RevModPhys.93.025010

[50] R. L. Workman *et al.* [Particle Data Group], "Review of Particle Physics," PTEP **2022**, 083C01 (2022) doi:10.1093/ptep/ptac097

[51] M. Ablikim *et al.* [BESIII], "Precision measurement of the mass of the τ lepton," Phys. Rev. D **90**, no.1, 012001 (2014) doi:10.1103/PhysRevD.90.012001 [arXiv:1405.1076 [hep-ex]].

[52] P. A. R. Ade *et al.* [Planck], "Planck 2015 results. XIII. Cosmological parameters," Astron. Astrophys. **594**, A13 (2016) doi:10.1051/0004-6361/201525830 [arXiv:1502.01589 [astro-ph.CO]].

[53] W. Altmannshofer and J. Zupan, "Snowmass White Paper: Flavor Model Building," [arXiv:2203.07726 [hep-ph]].

[54] L. Wolfenstein, "Parametrization of the Kobayashi-Maskawa Matrix," Phys. Rev. Lett. **51**, 1945 (1983) doi:10.1103/PhysRevLett.51.1945

[55] W. Altmannshofer *et al.* [PIONEER], "PIONEER: Studies of Rare Pion Decays," [arXiv:2203.01981 [hep-ex]].

[56] B. Belfatto, R. Beradze and Z. Berezhiani, "The CKM unitarity problem: A trace of new physics at the TeV scale?," Eur. Phys. J. C **80**, no.2, 149 (2020) doi:10.1140/epjc/s10052-020-7691-6 [arXiv:1906.02714 [hep-ph]].

[57] D. Bryman, V. Cirigliano, A. Crivellin and G. Inguglia, "Testing Lepton Flavor Universality with Pion, Kaon, Tau, and Beta Decays," Ann. Rev. Nucl. Part. Sci. **72**, 69-91 (2022) doi:10.1146/annurev-nucl-110121-051223 [arXiv:2111.05338 [hep-ph]].

[58] J. Charles *et al.* [CKMfitter], "CP violation and the CKM matrix: Assessing the impact of the asymmetric *B* factories," Eur. Phys. J. C **41**, no.1, 1-131 (2005) doi:10.1140/epjc/s2005-02169-1 [arXiv:hep-ph/0406184 [hep-ph]]. Online update at http://ckmfitter.in2p3.fr/

[59] M. Bona *et al.* [UTfit], "The Unitarity Triangle Fit in the Standard Model and Hadronic Parameters from Lattice QCD: A Reappraisal after the Measurements of ΔM_s and BR($B \to \tau\nu$)," JHEP **10**, 081 (2006) doi:10.1088/1126-6708/2006/10/081 [arXiv:hep-ph/0606167 [hep-ph]]. Online update at http://www.utfit.org/UTfit/

[60] M. Bona *et al.* [UTfit], "New UTfit Analysis of the Unitarity Triangle in the Cabibbo-Kobayashi-Maskawa scheme," Rend. Lincei Sci. Fis. Nat. **34**, 37-57 (2023) doi:10.1007/s12210-023-01137-5 [arXiv:2212.03894 [hep-ph]].

[61] C. D. Froggatt and H. B. Nielsen, "Hierarchy of Quark Masses, Cabibbo Angles and CP Violation," Nucl. Phys. B **147**, 277-298 (1979) doi:10.1016/0550-3213(79)90316-X

[62] N. Arkani-Hamed and M. Schmaltz, "Hierarchies without symmetries from extra dimensions," Phys. Rev. D **61**, 033005 (2000) doi:10.1103/PhysRevD.61.033005 [arXiv:hep-ph/9903417 [hep-ph]].

[63] Y. Grossman and M. Neubert, "Neutrino masses and mixings in nonfactorizable geometry," Phys. Lett. B **474**, 361-371 (2000) doi:10.1016/S0370-2693(00)00054-X [arXiv:hep-ph/9912408 [hep-ph]].

[64] T. Gherghetta and A. Pomarol, "Bulk fields and supersymmetry in a slice of AdS," Nucl. Phys. B **586**, 141-162 (2000) doi:10.1016/S0550-3213(00)00392-8 [arXiv:hep-ph/0003129 [hep-ph]].

[65] D. B. Kaplan, "Flavor at SSC energies: A New mechanism for dynamically generated fermion masses," Nucl. Phys. B **365**, 259-278 (1991) doi:10.1016/S0550-3213(05)80021-5

[66] S. Weinberg, "Electromagnetic and weak masses," Phys. Rev. Lett. **29**, 388-392 (1972) doi:10.1103/PhysRevLett.29.388

[67] M. Leurer, Y. Nir and N. Seiberg, "Mass matrix models: The Sequel," Nucl. Phys. B **420**, 468-504 (1994) doi:10.1016/0550-3213(94)90074-4 [arXiv:hep-ph/9310320 [hep-ph]].

[68] T. Blake, G. Lanfranchi and D. M. Straub, "Rare B Decays as Tests of the Standard Model," Prog. Part. Nucl. Phys. **92**, 50-91 (2017) doi:10.1016/j.ppnp.2016.10.001 [arXiv:1606.00916 [hep-ph]].

[69] W. Altmannshofer and F. Archilli, "Rare decays of b and c hadrons," [arXiv:2206.11331 [hep-ph]].

[70] A. Sirlin, "Large m_W, m_Z Behavior of the $O(\alpha)$ Corrections to Semileptonic Processes Mediated by W," Nucl. Phys. B **196**, 83-92 (1982) doi:10.1016/0550-3213(82)90303-0

[71] T. Inami and C. S. Lim, "Effects of Superheavy Quarks and Leptons in Low-Energy Weak Processes $K_L \to \mu\bar{\mu}$, $K^+ \to \pi^+\nu\bar{\nu}$ and $K^0 \leftrightarrow \bar{K}^0$," Prog. Theor. Phys. **65**, 297 (1981) [erratum: Prog. Theor. Phys. **65**, 1772 (1981)] doi:10.1143/PTP.65.297

[72] G. Buchalla, A. J. Buras and M. E. Lautenbacher, "Weak decays beyond leading logarithms," Rev. Mod. Phys. **68**, 1125-1144 (1996) doi:10.1103/RevModPhys.68.1125 [arXiv:hep-ph/9512380 [hep-ph]].

[73] C. Bobeth, M. Gorbahn, T. Hermann, M. Misiak, E. Stamou and M. Steinhauser, "$B_{s,d} \to l^+l^-$ in the Standard Model with Reduced Theoretical Uncertainty," Phys. Rev. Lett. **112**, 101801 (2014) doi:10.1103/PhysRevLett.112.101801 [arXiv:1311.0903 [hep-ph]].

[74] M. Beneke, C. Bobeth and R. Szafron, "Power-enhanced leading-logarithmic QED corrections to $B_q \to \mu^+\mu^-$," JHEP **10**, 232 (2019) [erratum: JHEP **11**, 099 (2022)] doi:10.1007/JHEP10(2019)232 [arXiv:1908.07011 [hep-ph]].

[75] K. De Bruyn, R. Fleischer, R. Knegjens, P. Koppenburg, M. Merk and N. Tuning, "Branching Ratio Measurements of B_s Decays," Phys. Rev. D **86**, 014027 (2012) doi:10.1103/PhysRevD.86.014027 [arXiv:1204.1735 [hep-ph]].

[76] V. Khachatryan *et al.* [CMS and LHCb], "Observation of the rare $B_s^0 \to \mu^+\mu^-$ decay from the combined analysis of CMS and LHCb data," Nature **522**, 68-72 (2015) doi:10.1038/nature14474 [arXiv:1411.4413 [hep-ex]].

[77] T. Blake, T. Gershon and G. Hiller, "Rare b hadron decays at the LHC," Ann. Rev. Nucl. Part. Sci. **65**, 113-143 (2015) doi:10.1146/annurev-nucl-102014-022231 [arXiv:1501.03309 [hep-ex]].

[78] S. Jäger and J. Martin Camalich, "On $B \to V\ell\ell$ at small dilepton invariant mass, power corrections, and new physics," JHEP **05**, 043 (2013) doi:10.1007/JHEP05(2013)043 [arXiv:1212.2263 [hep-ph]].

[79] N. Gubernari, D. van Dyk and J. Virto, "Non-local matrix elements in $B_{(s)} \to \{K^{(*)}, \phi\}\ell^+\ell^-$," JHEP **02**, 088 (2021) doi:10.1007/JHEP02(2021)088 [arXiv:2011.09813 [hep-ph]].

[80] G. Hiller and F. Kruger, "More model-independent analysis of $b \to s$ processes," Phys. Rev. D **69**, 074020 (2004) doi:10.1103/PhysRevD.69.074020 [arXiv:hep-ph/0310219 [hep-ph]].

[81] M. Bordone, G. Isidori and A. Pattori, "On the Standard Model predictions for R_K and R_{K^*}," Eur. Phys. J. C **76**, no.8, 440 (2016) doi:10.1140/epjc/s10052-016-4274-7 [arXiv:1605.07633 [hep-ph]].

[82] R. Aaij *et al.* [LHCb], "Test of lepton universality with $B^0 \to K^{*0}\ell^+\ell^-$ decays," JHEP **08**, 055 (2017) doi:10.1007/JHEP08(2017)055 [arXiv:1705.05802 [hep-ex]].

[83] R. Aaij *et al.* [LHCb], "Test of lepton universality in beauty-quark decays," Nature Phys. **18**, no.3, 277-282 (2022) doi:10.1038/s41567-021-01478-8 [arXiv:2103.11769 [hep-ex]].

[84] LHCb collaboration, "Test of lepton universality in $b \to s\ell^+\ell^-$ decays," [arXiv:2212.09152 [hep-ex]].

[85] LHCb collaboration, "Measurement of lepton universality parameters in $B^+ \to K^+\ell^+\ell^-$ and $B^0 \to K^{*0}\ell^+\ell^-$ decays," [arXiv:2212.09153 [hep-ex]].

[86] E. Waheed *et al.* [Belle], "Measurement of the CKM matrix element $|V_{cb}|$ from $B^0 \to D^{*-}\ell^+\nu_\ell$ at Belle," Phys. Rev. D **100**, no.5, 052007 (2019) [erratum: Phys. Rev. D **103**, no.7, 079901 (2021)] doi:10.1103/PhysRevD.100.052007 [arXiv:1809.03290 [hep-ex]].

[87] F. U. Bernlochner, Z. Ligeti, M. Papucci and D. J. Robinson, "Combined analysis of semileptonic B decays to D and D^*: $R(D^{(*)})$, $|V_{cb}|$, and new physics," Phys. Rev. D **95**, no.11, 115008 (2017) [erratum: Phys. Rev. D **97**, no.5, 059902 (2018)] doi:10.1103/PhysRevD.95.115008 [arXiv:1703.05330 [hep-ph]].

[88] J. P. Lees *et al.* [BaBar], "Evidence for an excess of $\bar{B} \to D^{(*)}\tau^-\bar{\nu}_\tau$ decays," Phys. Rev. Lett. **109**, 101802 (2012) doi:10.1103/PhysRevLett.109.101802 [arXiv:1205.5442 [hep-ex]].

[89] S. Descotes-Genon, J. Matias, M. Ramon and J. Virto, "Implications from clean observables for the binned analysis of $B \to K * \mu^+\mu^-$ at large recoil," JHEP **01**, 048 (2013) doi:10.1007/JHEP01(2013)048 [arXiv:1207.2753 [hep-ph]].

[90] A. Khodjamirian, T. Mannel, A. A. Pivovarov and Y. M. Wang, "Charm-loop effect in $B \to K^{(*)}\ell^+\ell^-$ and $B \to K^*\gamma$," JHEP **09**, 089 (2010) doi:10.1007/JHEP09(2010)089 [arXiv:1006.4945 [hep-ph]].

[91] C. Bobeth, M. Chrzaszcz, D. van Dyk and J. Virto, "Long-distance effects in $B \to K^*\ell\ell$ from analyticity," Eur. Phys. J. C **78**, no.6, 451 (2018) doi:10.1140/epjc/s10052-018-5918-6 [arXiv:1707.07305 [hep-ph]].

[92] T. Blake, U. Egede, P. Owen, K. A. Petridis and G. Pomery, "An empirical model to determine the hadronic resonance contributions to $\overline{B}^0 \to \overline{K}^{*0}\mu^+\mu^-$ transitions," Eur. Phys. J. C **78**, no.6, 453 (2018) doi:10.1140/epjc/s10052-018-5937-3 [arXiv:1709.03921 [hep-ph]].

[93] N. Gubernari, M. Reboud, D. van Dyk and J. Virto, "Improved theory predictions and global analysis of exclusive $b \to s\mu^+\mu^-$ processes," JHEP **09**, 133 (2022) doi:10.1007/JHEP09(2022)133 [arXiv:2206.03797 [hep-ph]].

[94] D. M. Straub, "flavio: a Python package for flavour and precision phenomenology in the Standard Model and beyond," [arXiv:1810.08132 [hep-ph]].

[95] W. Altmannshofer, S. A. Gadam and S. Profumo, "Probing New Physics with $\mu^+\mu^- \to bs$ at a Muon Collider," [arXiv:2306.15017 [hep-ph]].

[96] L. S. Geng, B. Grinstein, S. Jäger, S. Y. Li, J. Martin Camalich and R. X. Shi, "Implications of new evidence for lepton-universality violation in $b \to s\ell^+\ell^-$ decays," Phys. Rev. D **104**, no.3, 035029 (2021) doi:10.1103/PhysRevD.104.035029 [arXiv:2103.12738 [hep-ph]].

[97] W. Altmannshofer and P. Stangl, "New physics in rare B decays after Moriond 2021," Eur. Phys. J. C **81**, no.10, 952 (2021) doi:10.1140/epjc/s10052-021-09725-1 [arXiv:2103.13370 [hep-ph]].

[98] T. Hurth, F. Mahmoudi, D. M. Santos and S. Neshatpour, "More Indications for Lepton Nonuniversality in $b \to s\ell^+\ell^-$," Phys. Lett. B **824**, 136838 (2022) doi:10.1016/j.physletb.2021.136838 [arXiv:2104.10058 [hep-ph]].

[99] M. Ciuchini, M. Fedele, E. Franco, A. Paul, L. Silvestrini and M. Valli, "Constraints on lepton universality violation from rare B decays," Phys. Rev. D **107**, no.5, 055036 (2023) doi:10.1103/PhysRevD.107.055036 [arXiv:2212.10516 [hep-ph]].

[100] M. Algueró, A. Biswas, B. Capdevila, S. Descotes-Genon, J. Matias and M. Novoa-Brunet, "To (b)e or not to (b)e: no electrons at LHCb," Eur. Phys. J. C **83**, no.7, 648 (2023) doi:10.1140/epjc/s10052-023-11824-0 [arXiv:2304.07330 [hep-ph]].

[101] K. S. M. Lee, Z. Ligeti, I. W. Stewart and F. J. Tackmann, "Extracting short distance information from $b \to sl^+l^-$ effectively," Phys. Rev. D **75**, 034016 (2007) doi:10.1103/PhysRevD.75.034016 [arXiv:hep-ph/0612156 [hep-ph]].

[102] T. Huber, T. Hurth, J. Jenkins, E. Lunghi, Q. Qin and K. K. Vos, "Phenomenology of inclusive $\overline{B} \to X_s\ell^+\ell^-$ for the Belle II era," JHEP **10**, 088 (2020) doi:10.1007/JHEP10(2020)088 [arXiv:2007.04191 [hep-ph]].

[103] A. V. Rusov, "Probing New Physics in $b \to d$ transitions," JHEP **07**, 158 (2020) doi:10.1007/JHEP07(2020)158 [arXiv:1911.12819 [hep-ph]].

[104] R. Bause, H. Gisbert, M. Golz and G. Hiller, "Model-independent analysis of $b \to d$ processes," Eur. Phys. J. C **83**, no.5, 419 (2023) doi:10.1140/epjc/s10052-023-11586-9 [arXiv:2209.04457 [hep-ph]].

[105] W. Altmannshofer, A. J. Buras, D. M. Straub and M. Wick, "New strategies for New Physics search in $B \to K^* \nu\bar{\nu}$, $B \to K\nu\bar{\nu}$ and $B \to X_s \nu\bar{\nu}$ decays," JHEP **04**, 022 (2009) doi:10.1088/1126-6708/2009/04/022 [arXiv:0902.0160 [hep-ph]].

[106] D. Bečirević, G. Piazza and O. Sumensari, "Revisiting $B \to K^{(*)} \nu\bar{\nu}$ decays in the Standard Model and beyond," Eur. Phys. J. C **83**, no.3, 252 (2023) doi:10.1140/epjc/s10052-023-11388-z [arXiv:2301.06990 [hep-ph]].

[107] J. F. Kamenik, S. Monteil, A. Semkiv and L. V. Silva, "Lepton polarization asymmetries in rare semi-tauonic $b \to s$ exclusive decays at FCC-ee," Eur. Phys. J. C **77**, no.10, 701 (2017) doi:10.1140/epjc/s10052-017-5272-0 [arXiv:1705.11106 [hep-ph]].

[108] L. Li and T. Liu, "$b \to s\tau^+\tau^-$ physics at future Z factories," JHEP **06**, 064 (2021) doi:10.1007/JHEP06(2021)064 [arXiv:2012.00665 [hep-ph]].

[109] G. y. Huang, S. Jana, F. S. Queiroz and W. Rodejohann, "Probing the $R_{K^{(*)}}$ anomaly at a muon collider," Phys. Rev. D **105**, no.1, 015013 (2022) doi:10.1103/PhysRevD.105.015013 [arXiv:2103.01617 [hep-ph]].

[110] P. Asadi, R. Capdevilla, C. Cesarotti and S. Homiller, "Searching for leptoquarks at future muon colliders," JHEP **10**, 182 (2021) doi:10.1007/JHEP10(2021)182 [arXiv:2104.05720 [hep-ph]].

[111] S. Qian, C. Li, Q. Li, F. Meng, J. Xiao, T. Yang, M. Lu and Z. You, "Searching for heavy leptoquarks at a muon collider," JHEP **12**, 047 (2021) doi:10.1007/JHEP12(2021)047 [arXiv:2109.01265 [hep-ph]].

[112] W. Altmannshofer, S. A. Gadam and S. Profumo, "Snowmass White Paper: Probing New Physics with $\mu^+\mu^- \to bs$ at a Muon Collider," [arXiv:2203.07495 [hep-ph]].

[113] A. Azatov, F. Garosi, A. Greljo, D. Marzocca, J. Salko and S. Trifinopoulos, "New physics in $b \to s\mu\mu$: FCC-hh or a muon collider?," JHEP **10**, 149 (2022) doi:10.1007/JHEP10(2022)149 [arXiv:2205.13552 [hep-ph]].